



M.N.Kiselev



Nanostructures

Carbon Nanotubes
Quantum Dots
Molecular Transistors

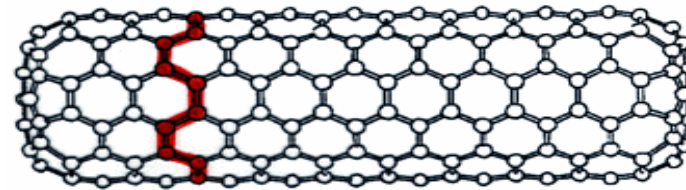
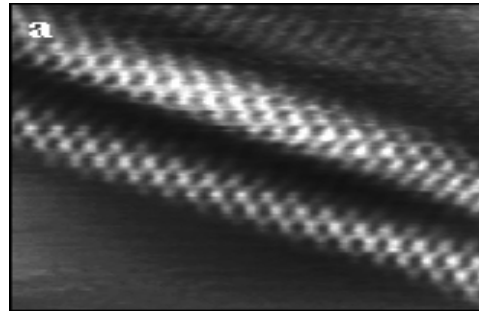


One-dimensional structures

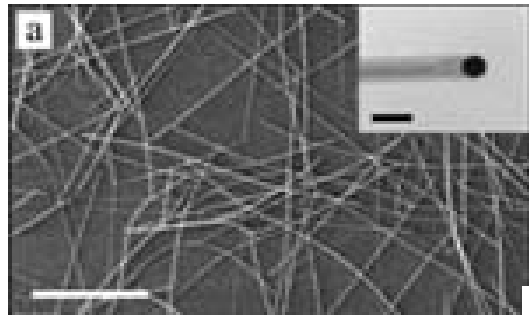
1D-Systems



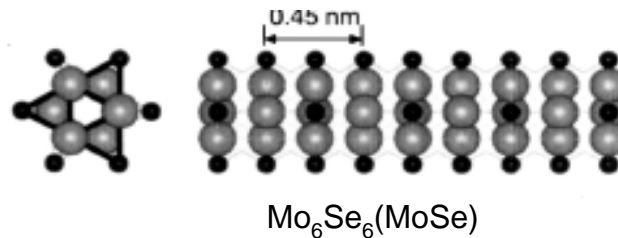
1D systems - Carbon Nanotubes



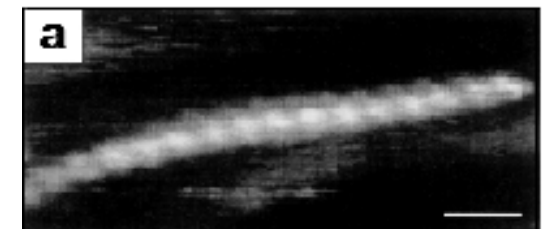
Semiconducting Nanowires



GaAs GaP InP InAs ZnS ZnSe CdS CdSe
GaAs_{0.6}P_{0.4} InAs_{0.5}P_{0.5} GaN(Fe)



Single molecules



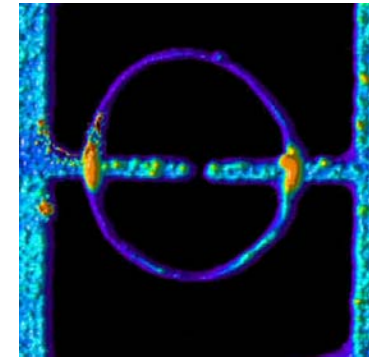
Carbon Nanotubes



■ Some Ideas:

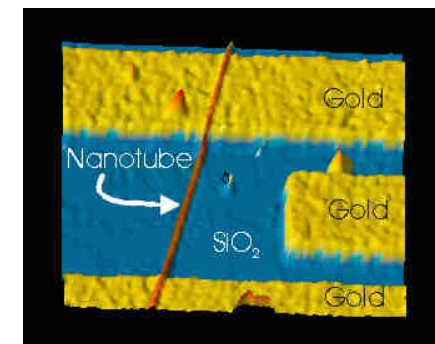
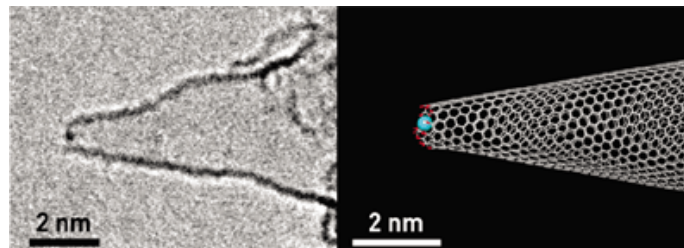
- Nanohorns (adsorptive and cathalytical properties → fuel cells)
- Nano test-tubes (tubes can be opened and filled, e.g. biological molecules)
- Nanofibres (CN are supposed to be very strong)
- Nanotube rings

- SC: electronic devices MOSFET (Silicon - CN), FET
- Small bandgap CN: 1d conductor

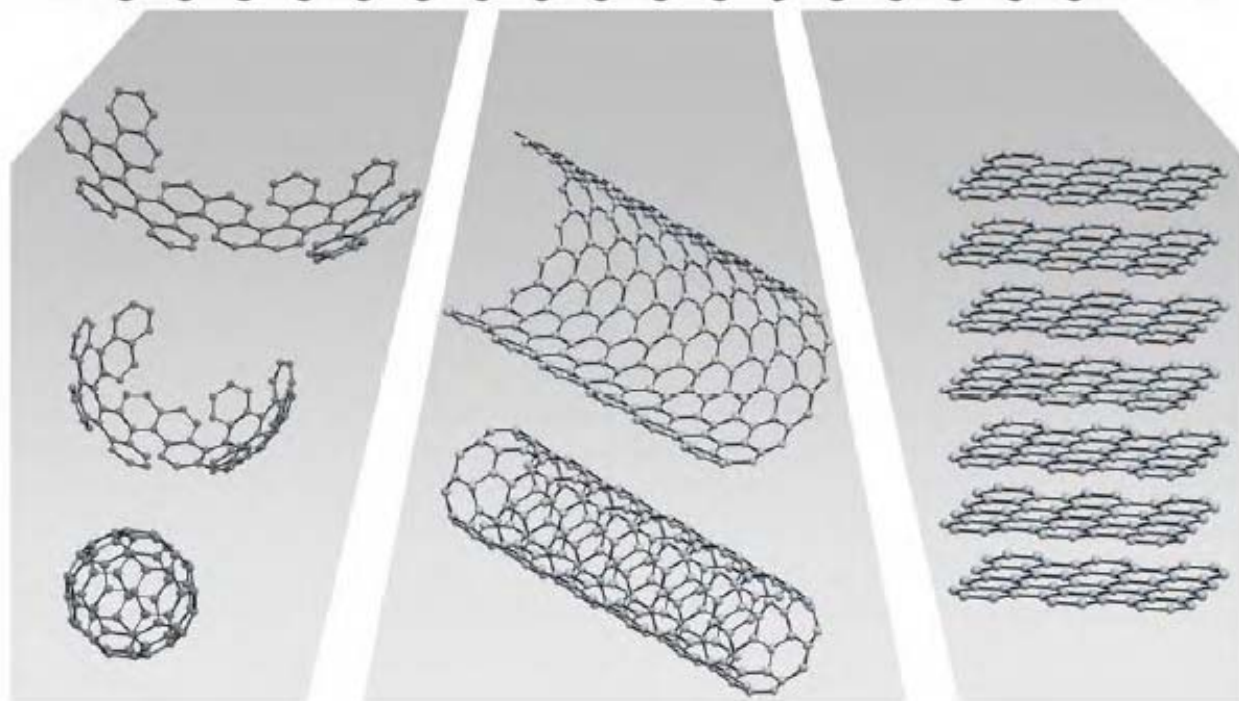
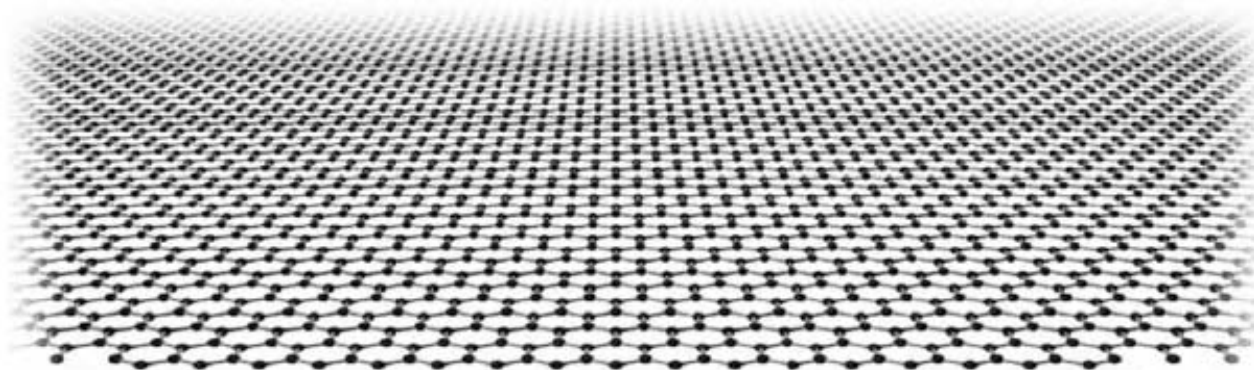


■ Model system for 1D transport

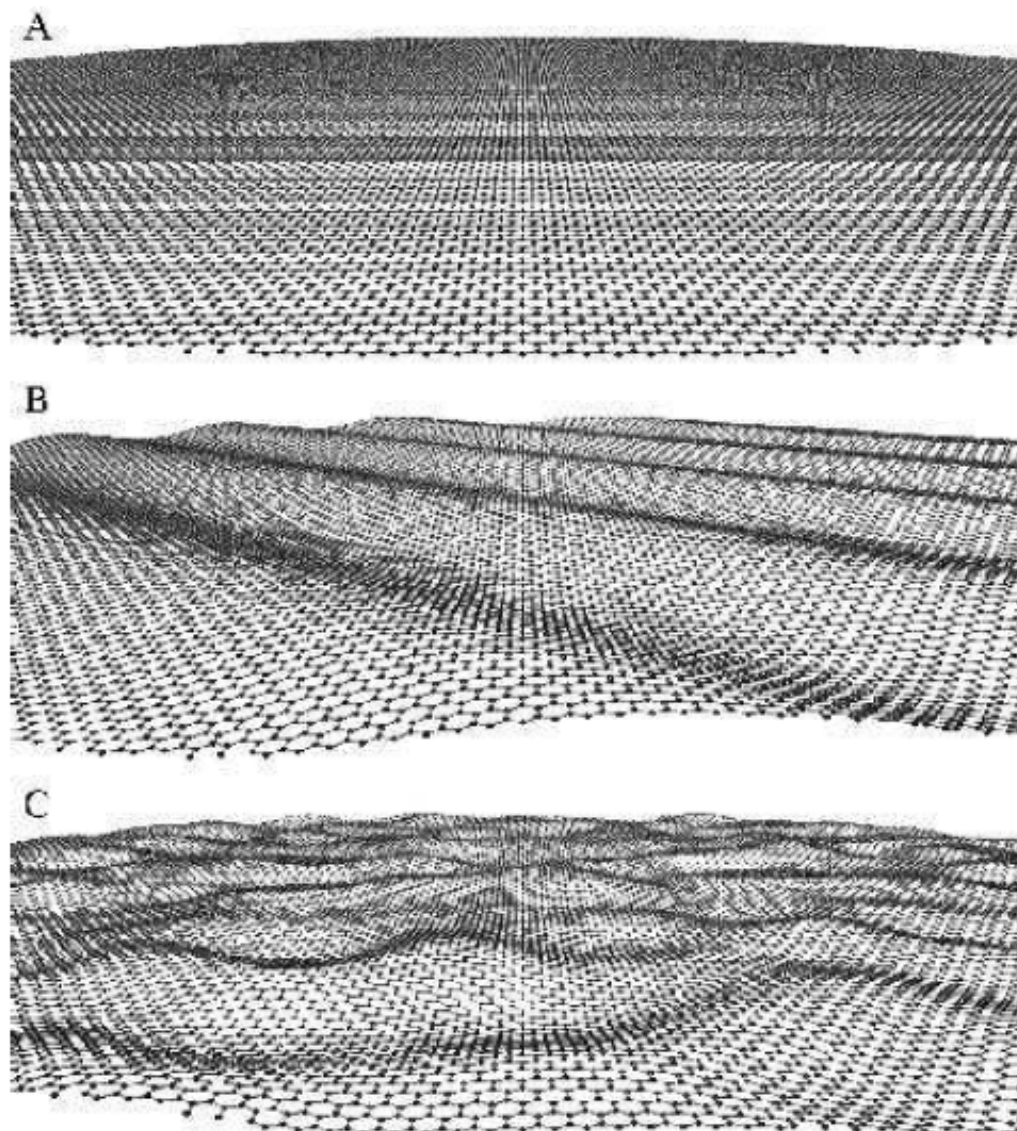
- Ballistic transport
- Little structural disorder
- $T \ll$ Coulomb diamonds



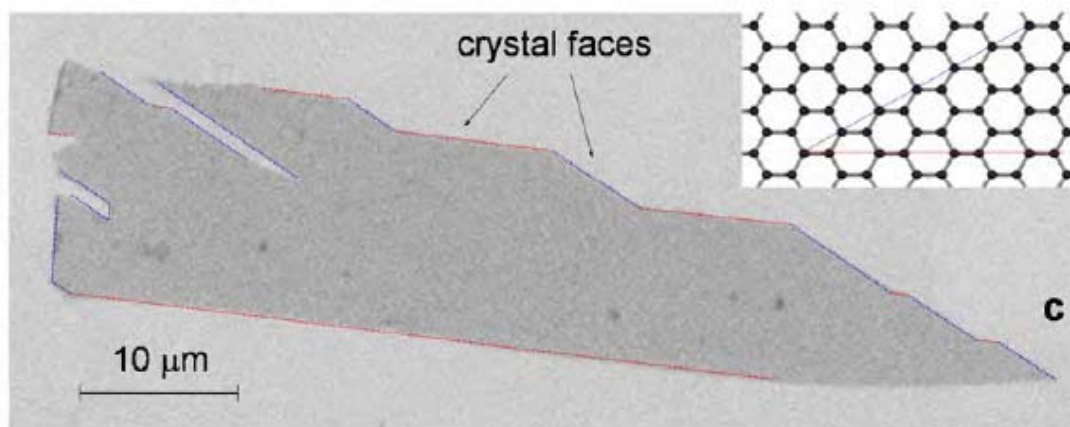
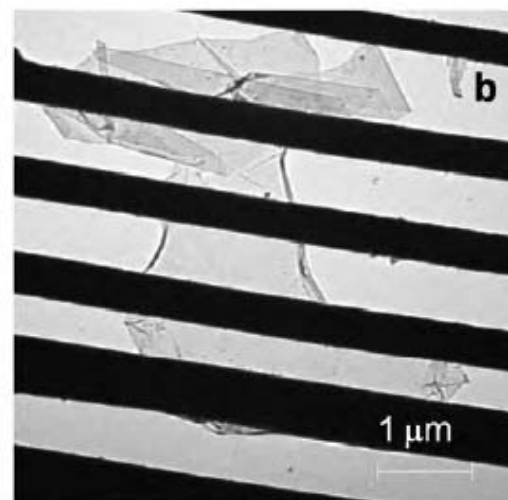
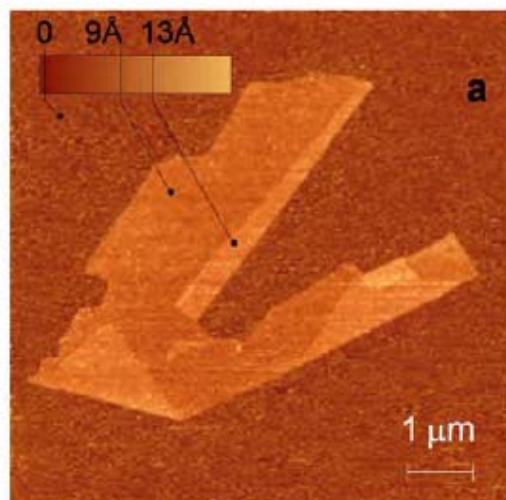
Graphene



Graphene



Graphene

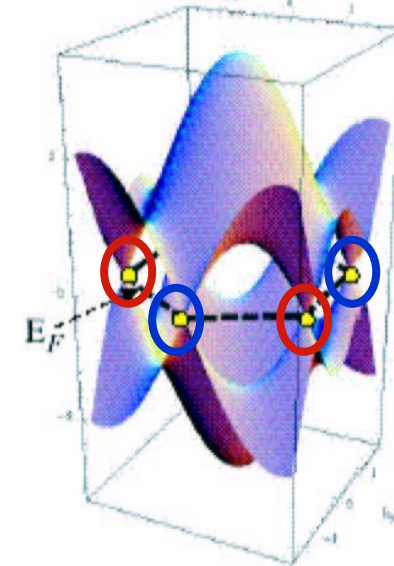
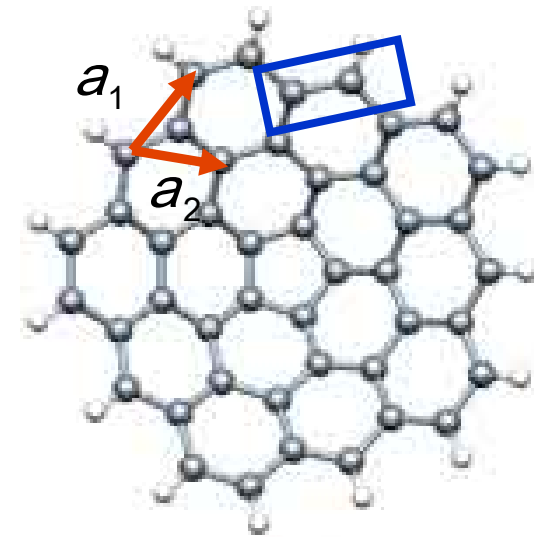


Graphene



Wallace, Phys. Rev. 71, 622 (1946)

- Structure:
 - Graphite sheet
 - hexagonal (honeycomb) lattice of C atoms
 - 2 atoms per unit cell
- Electron configuration:
 - 6 electrons: $1s^2, 2p_x, 2p_y = sp^2, 2p_z$
- Energy band structure:
 - most directions:
Electrons moving at E_F are backscattered
 - some directions:
Electrons may propagate

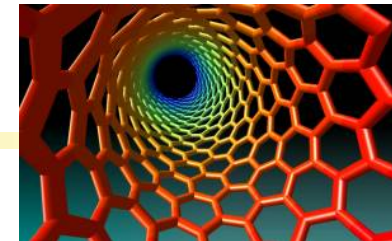


2 Fermi
points
 $K_{1,2}$

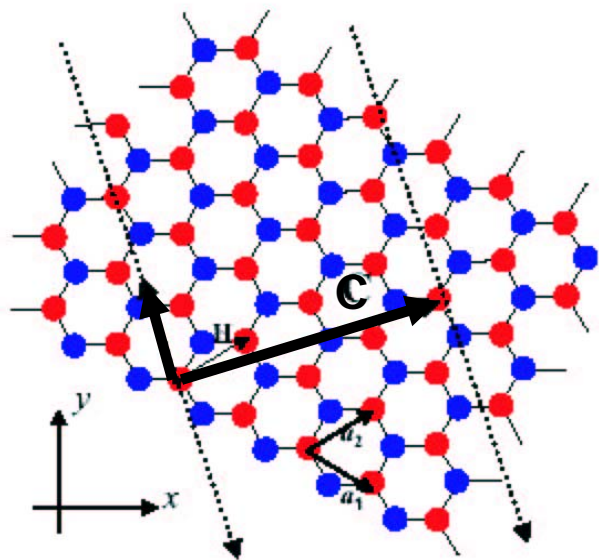


GRAPHENE is a SEMIMETAL

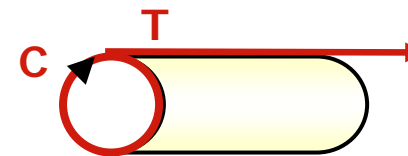
Graphene → Carbon Nanotubes



- Lattice of a Carbon Nanotube = rolled up graphite sheet



conformal mapping



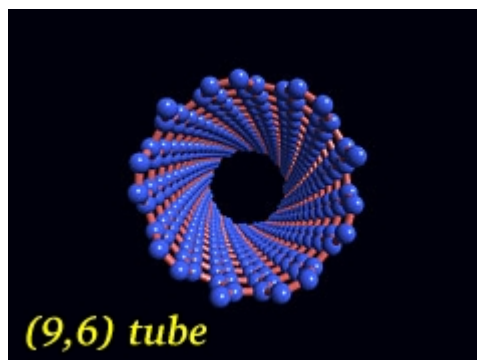
Periodic boundary condition

→ quantization of k_p

$$k_p = 2\pi n_c / C$$

Chiral vector $\vec{C} = n\vec{a}_1 + m\vec{a}_2$

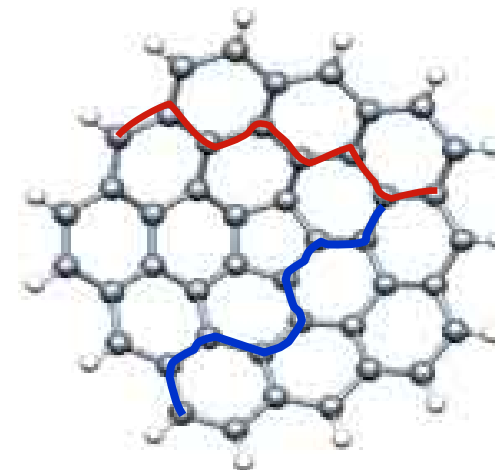
CN labeled
(n,m)



- 2 examples:

- Zigzag (n,0)

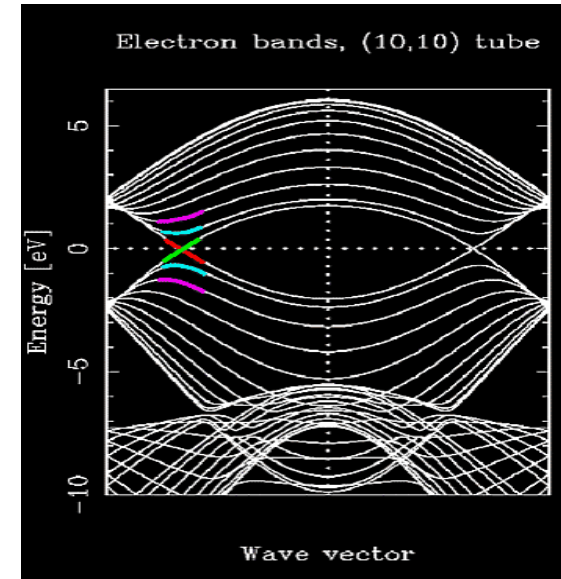
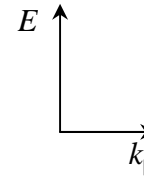
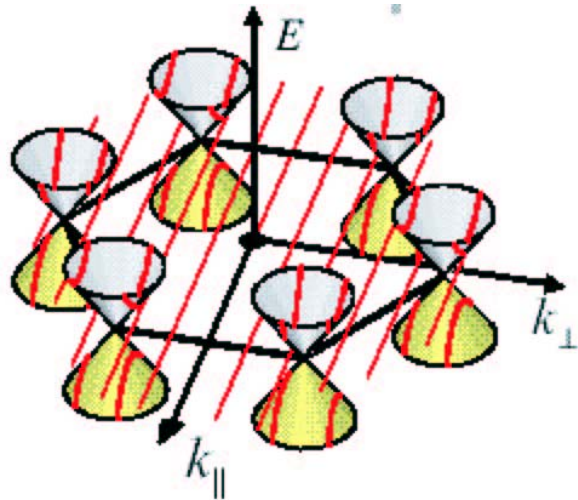
- Armchair (n,n)



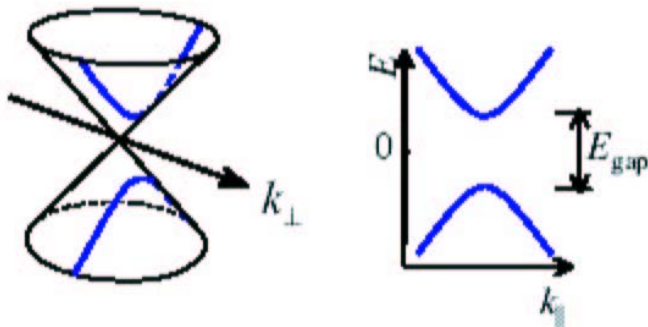
Bandstructure of CNs



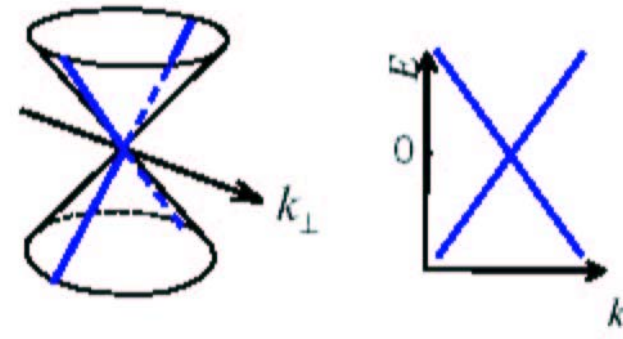
- Quantization of the SEMIMETAL Graphene



- SEMICONDUCTOR (2/3)



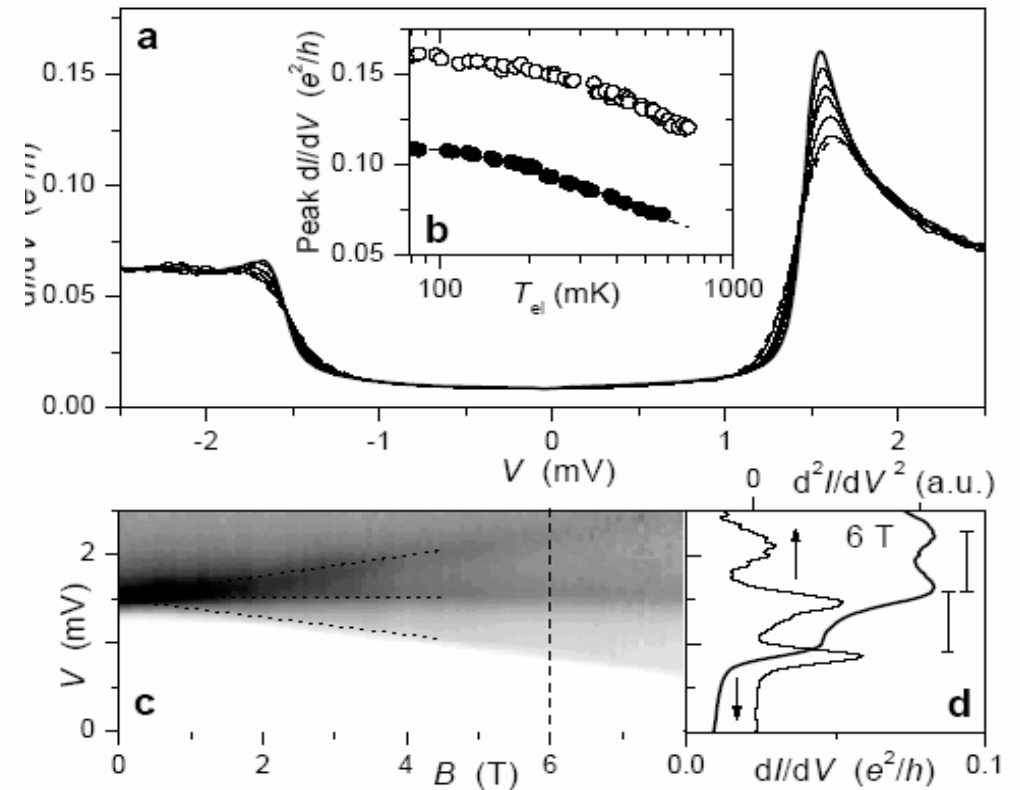
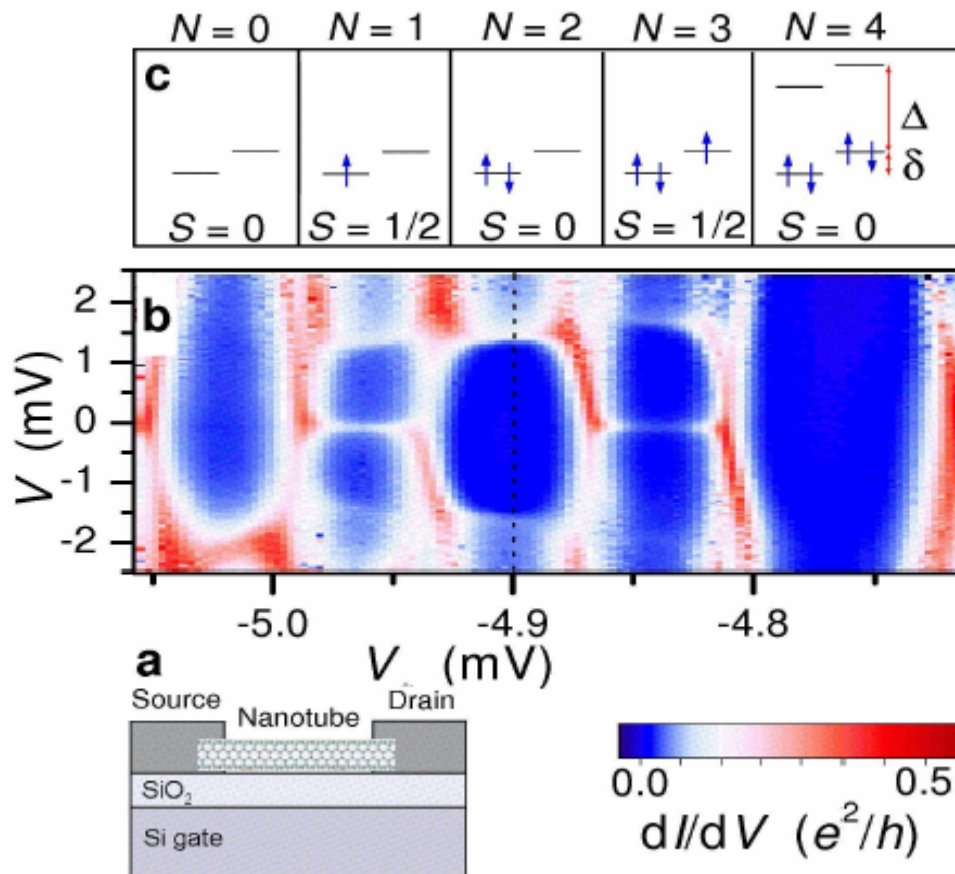
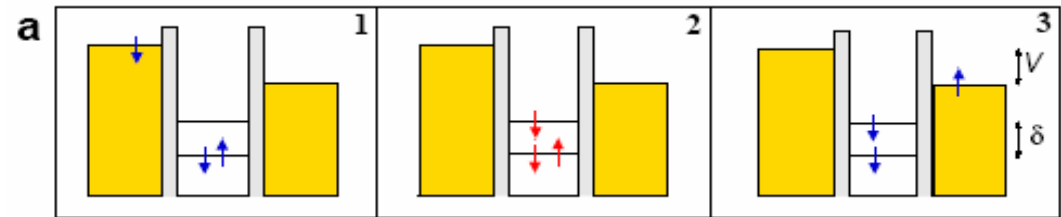
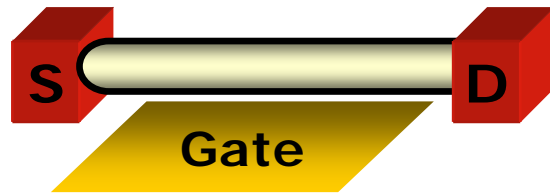
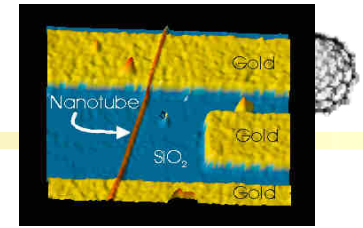
- "METAL" (1/3)



Examples:
Zigzag (n,0)
Armchair (n,n)

Semimetal Graphene → Quantization → Semiconducting and "metallic" CN

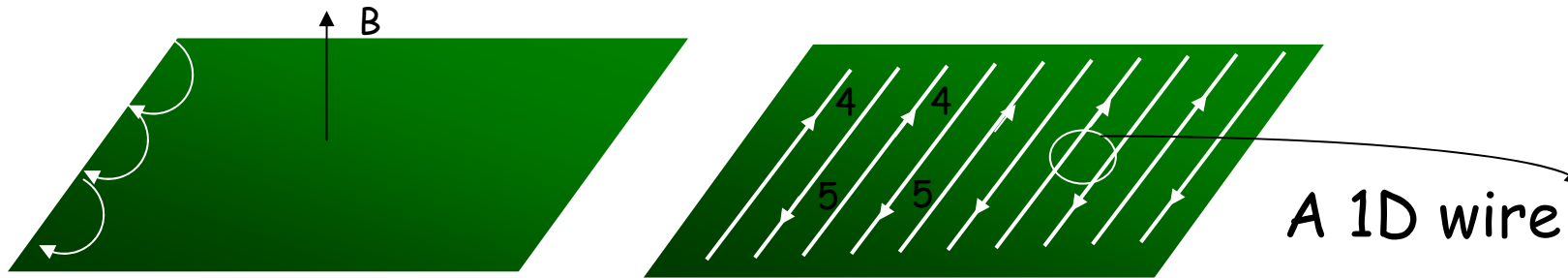
Transport through Carbon Nanotubes



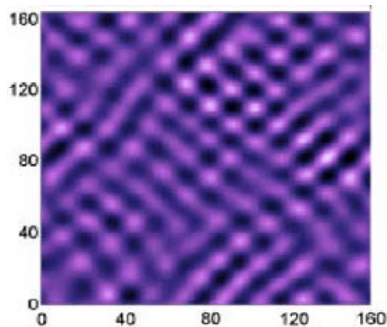
Other Systems Showing 1D Physics



2D systems - Chiral edges of the QH and FQHE
Striped phase at high Landau levels

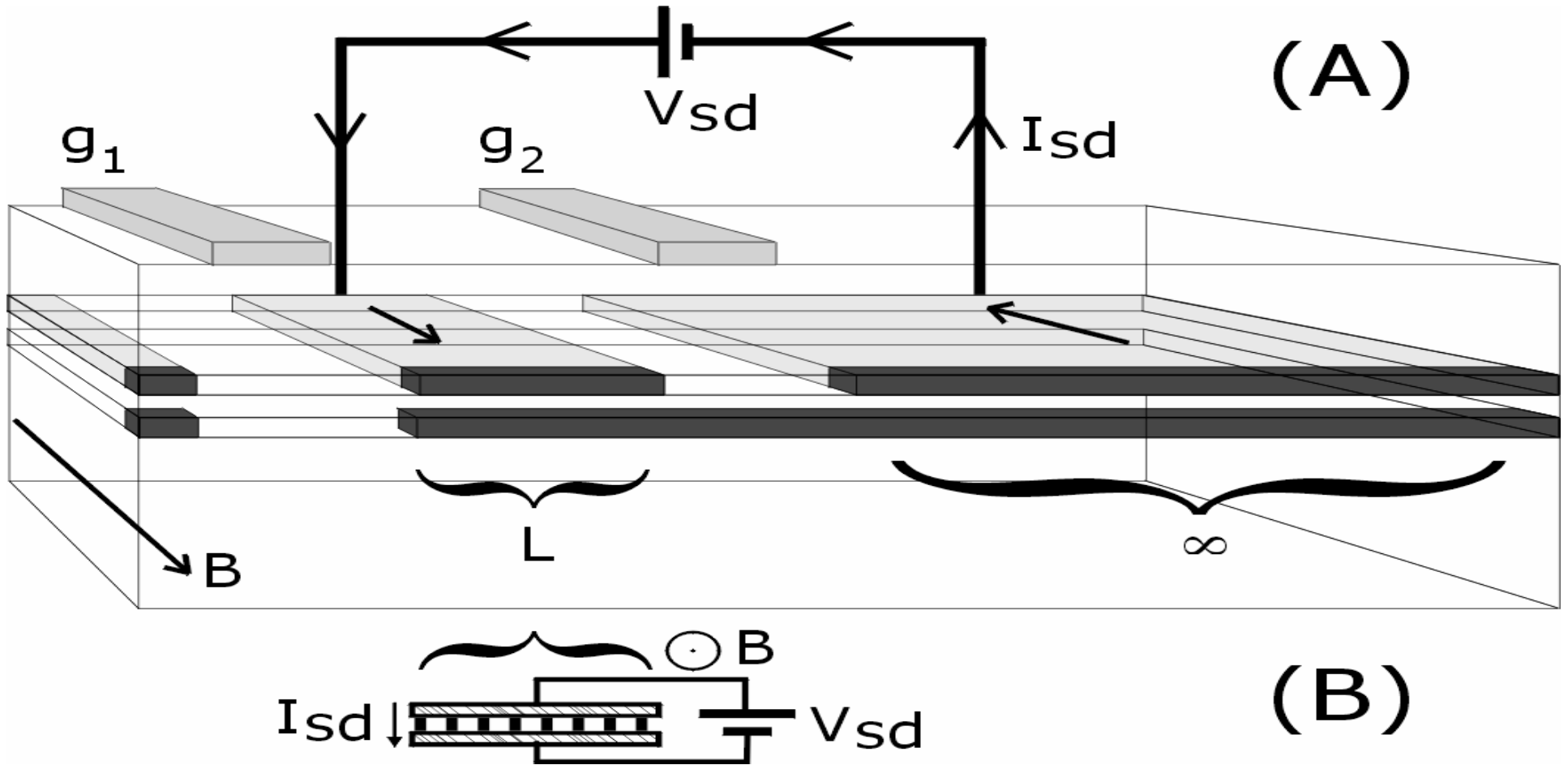


3D systems - Crystals of 1D molecules - Polyacetelene
Stripes in High Tc superconductors



Coupled wires systems

Circuit

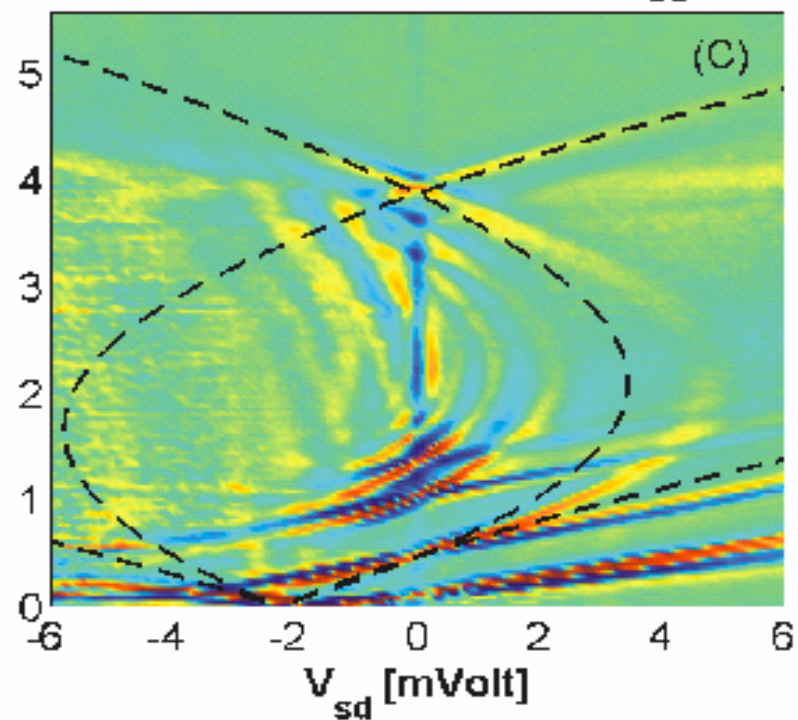
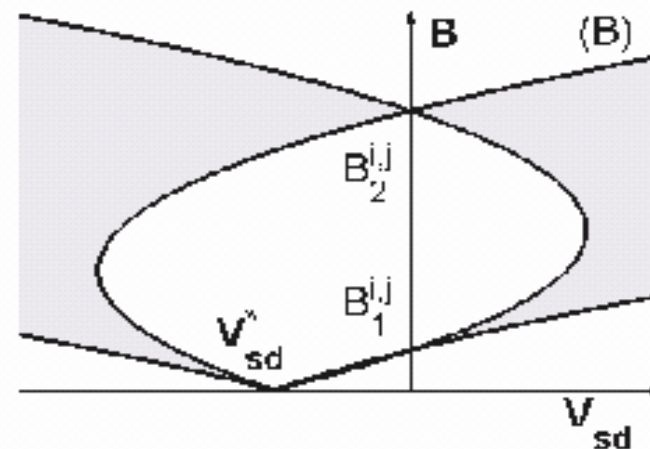
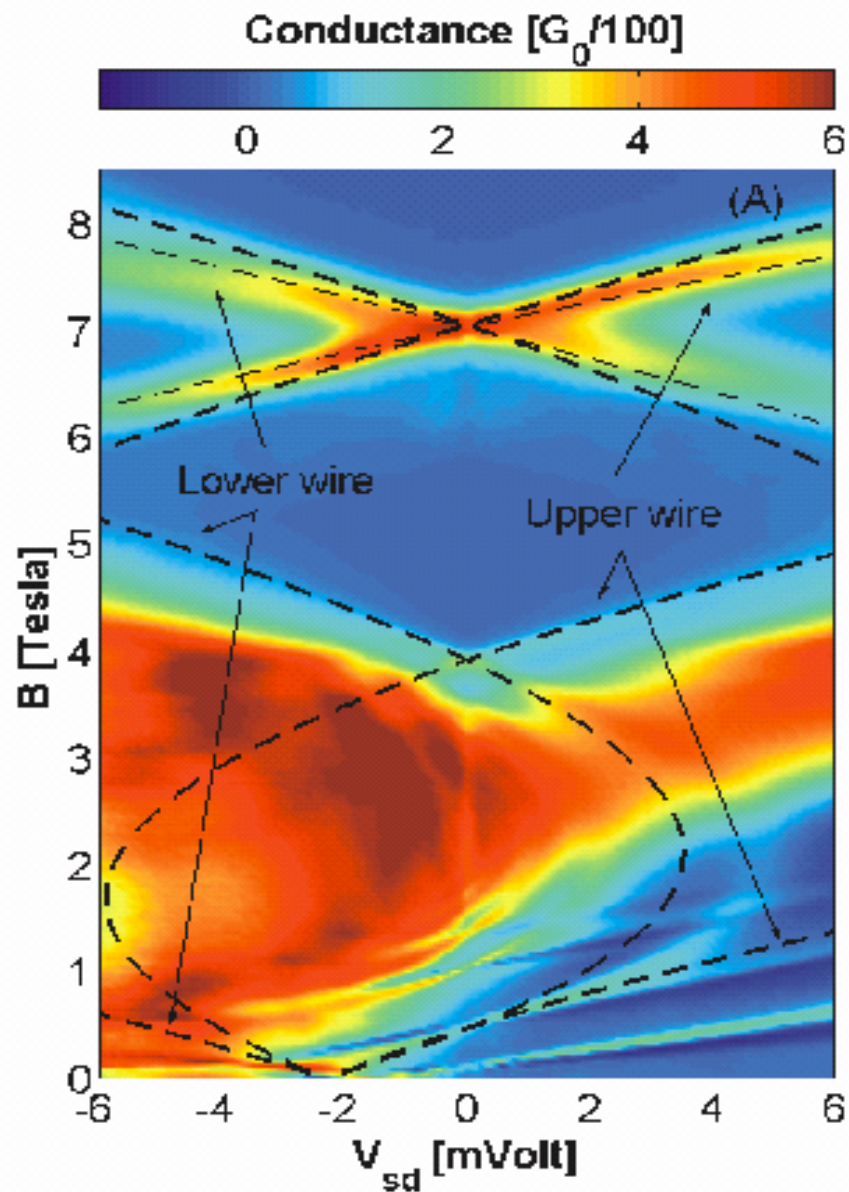


Top wire in equilibrium with the **source**
and bottom wire in equilibrium with the **drain**

Spin-Charge separation



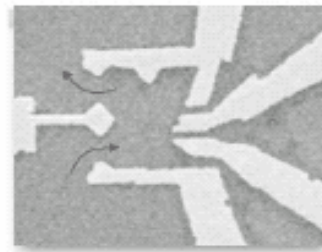
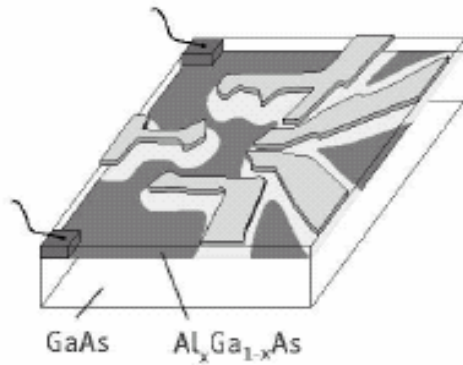
Observe 30% deviations



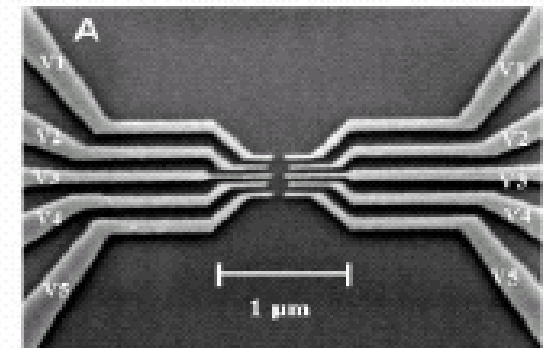
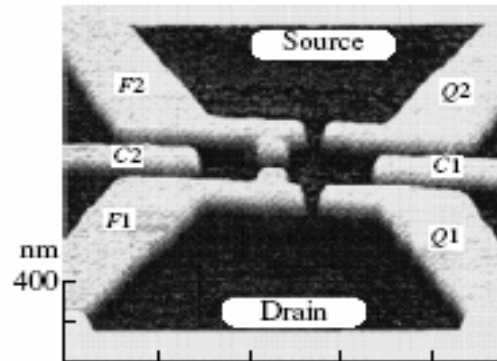
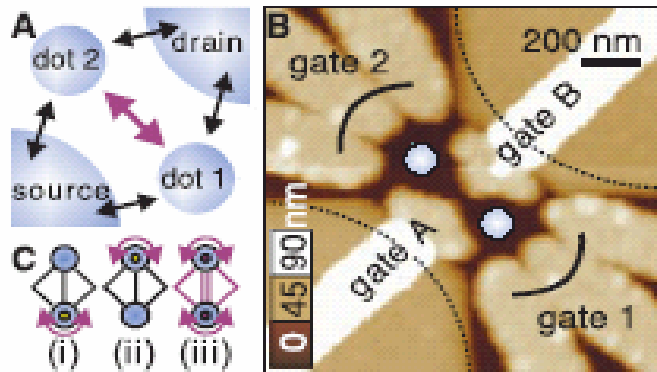
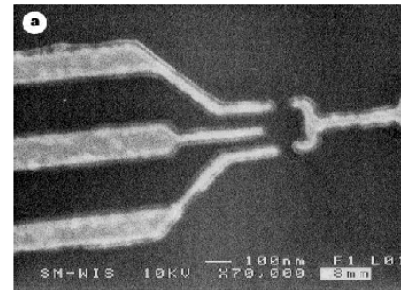


Zero-dimensional structures

Quantum dots: from simple to complex



1 μm



D.Goldhaber-Gordon et al (1998)

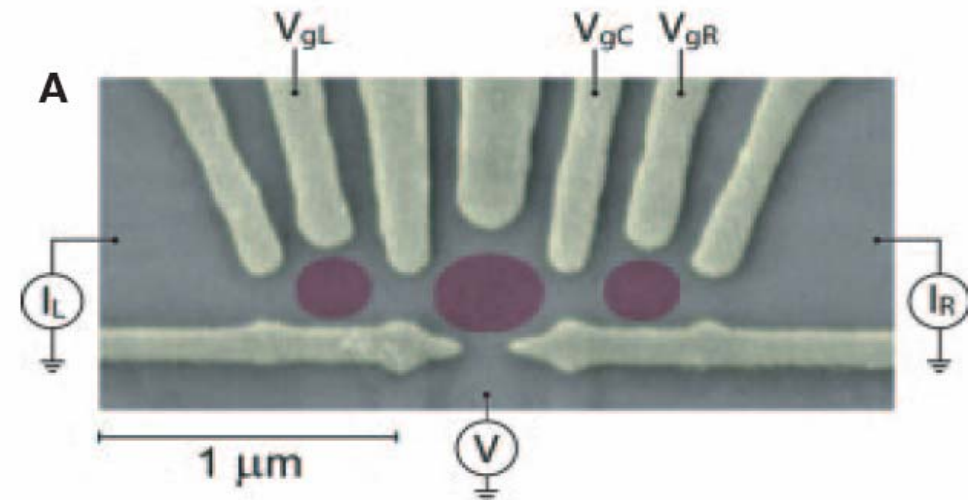
J.P.Kotthaus (1995)

A.Holleitner et al (2002)

L.W.Molenkamp et al (1995)

H.Jeong et al (2001)

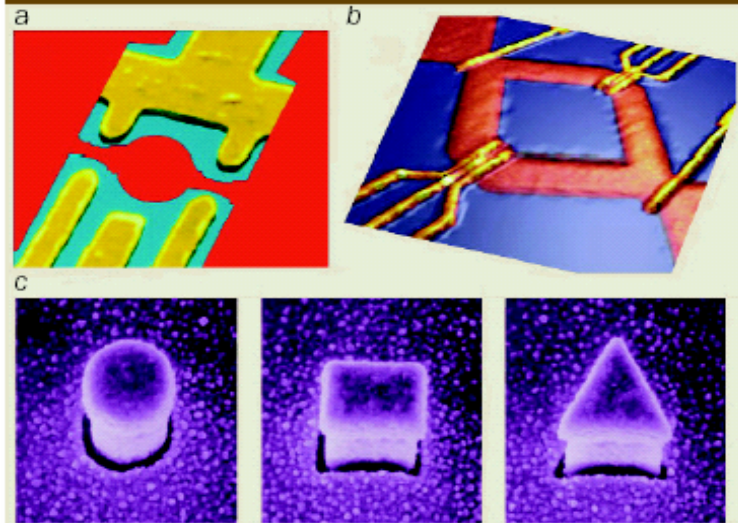
C.Marcus et al (2003)



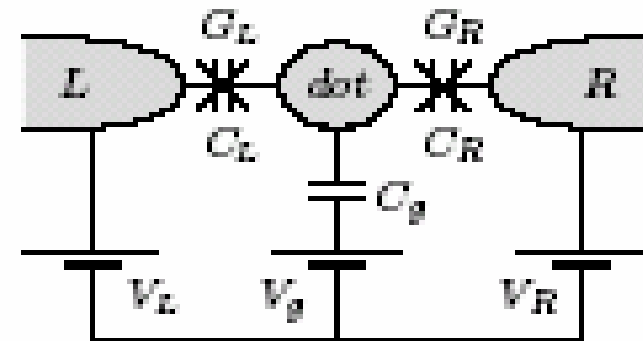
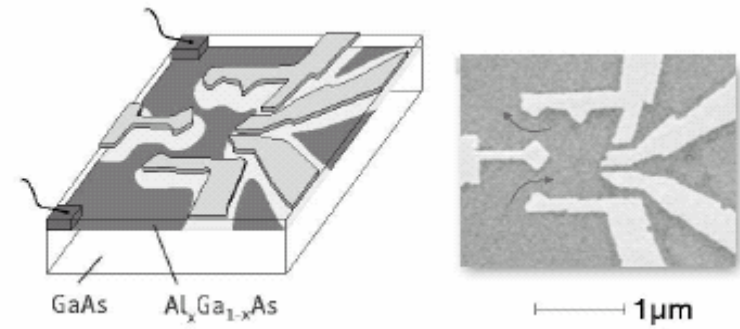
Quantum Dot devices



4 Quantum-dot devices

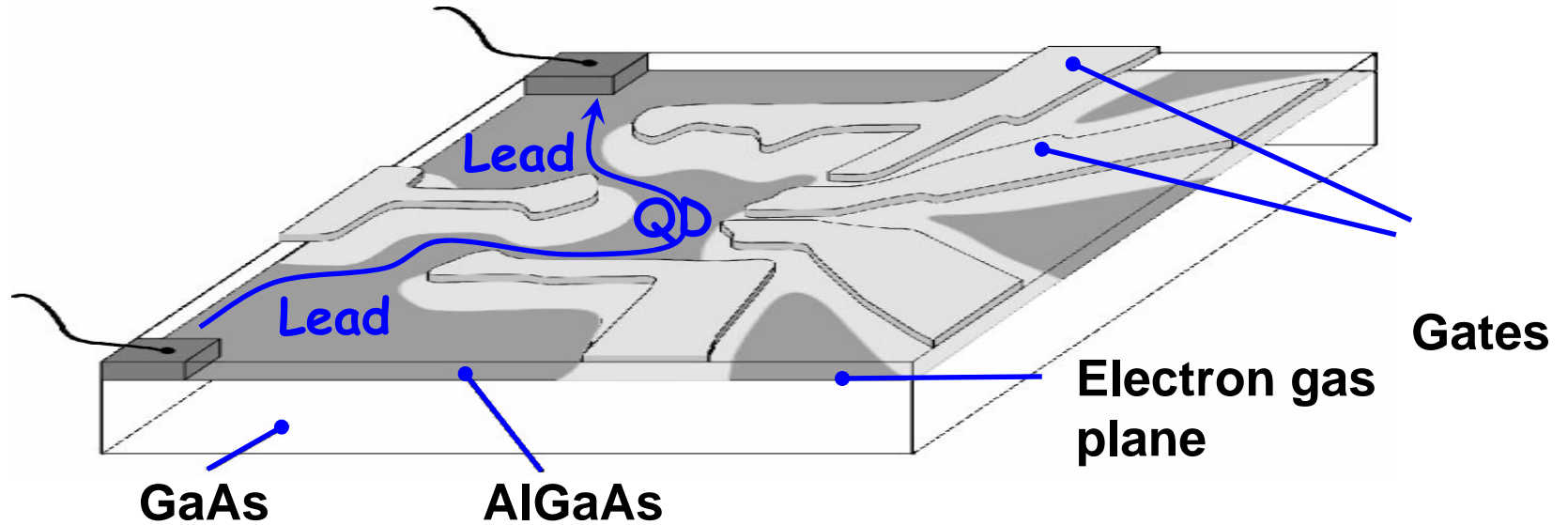


(a) A quantum dot can be defined by applying voltages to the surrounding gate electrodes (yellow). The tunnelling between the dot and the external electrodes (top left) is controlled by changing the voltages on the lower-left and lower-right gates. This coupling defines the lifetime broadening, Γ , of the quantum state in the dot. The number of electrons and the energy levels are tuned by the voltage on the lower-central gate. The puddle of electrons (confined red region) is about 0.5 microns in diameter. (b) Quantum dots can be placed in both arms of a two-slit interference device. Such a device has been used to investigate whether this scattering destroys the interference pattern. (c) Three quantum dots that have been used to compare the Kondo effect for singlet, doublet and triplet spin-states.



Artificial atoms

Quantum dots

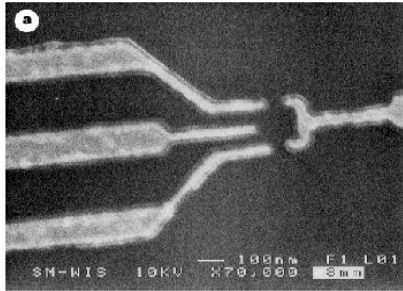


Tune: gate potentials, temperature, field...

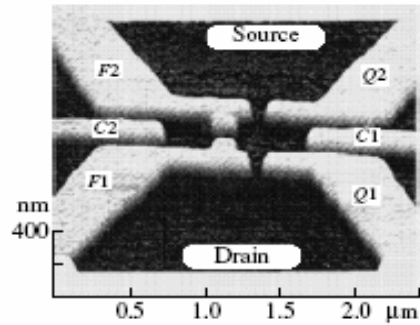
Measure: I-V curves, conductance G ...

Aharonov-Bohm interferometry, dephasing, coherent state manipulation...

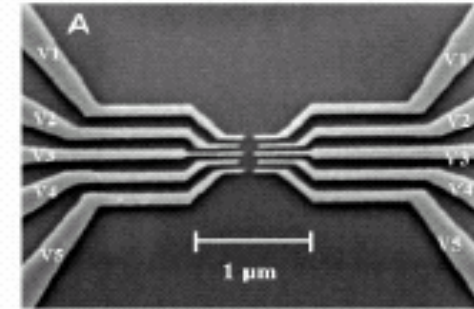
Coupled Quantum Dots



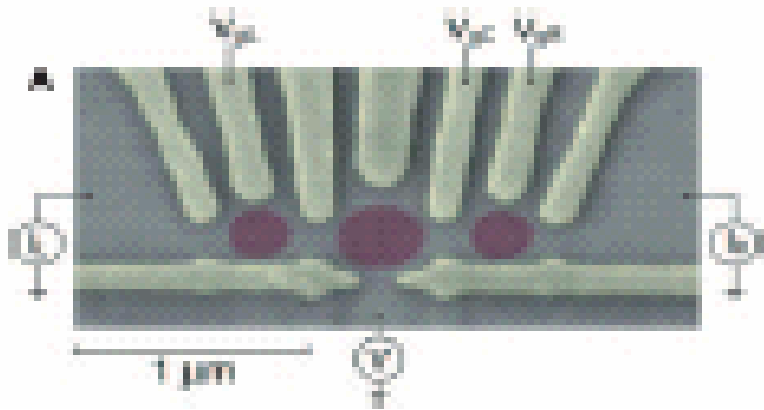
Single QD



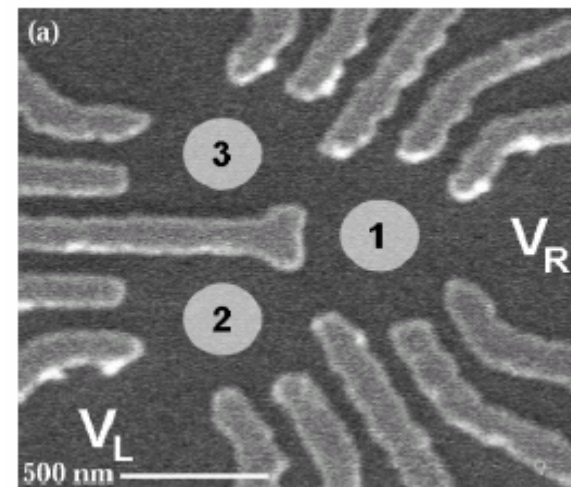
Double parallel QD



Double serial QD

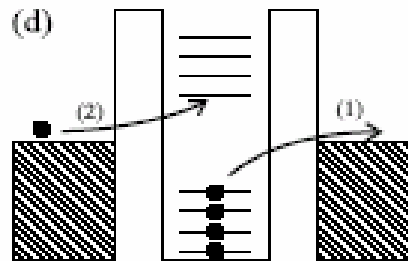
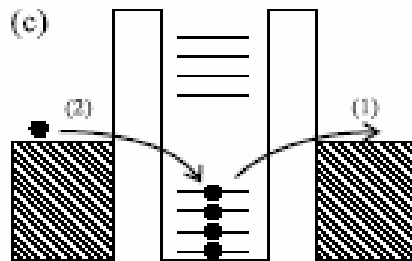
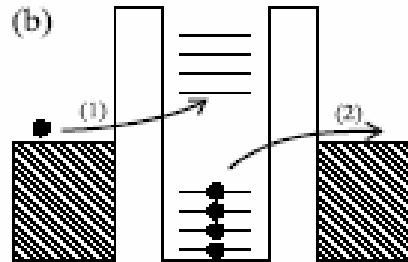
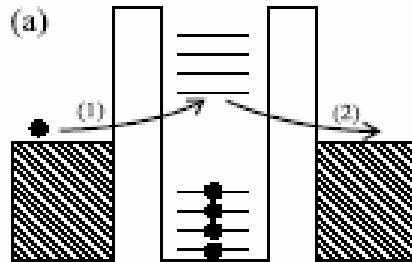
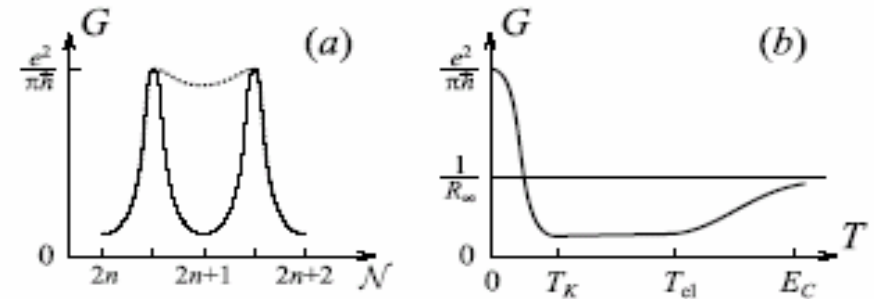
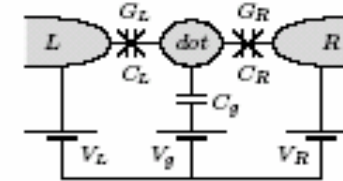
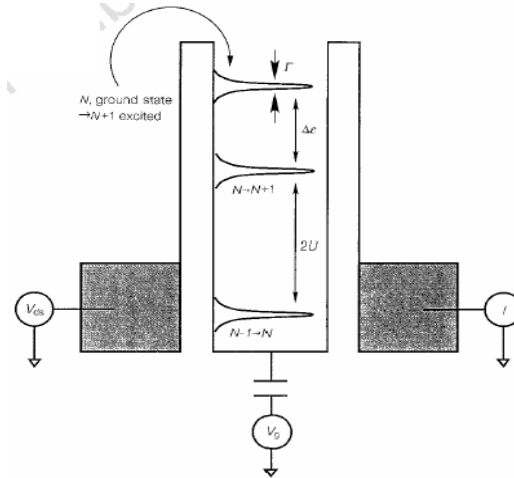
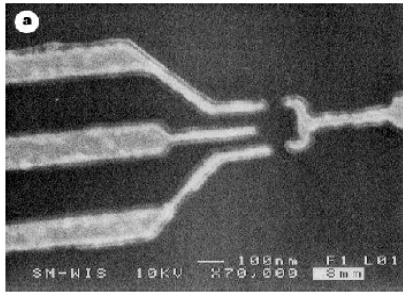


Triple serial QD



Triangular QD

Quantum Dots with few electrons

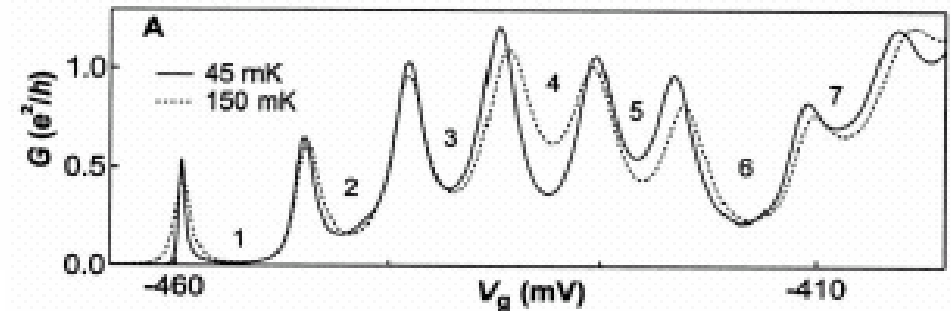


Elastic

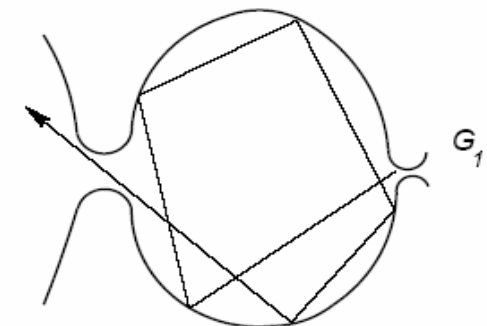
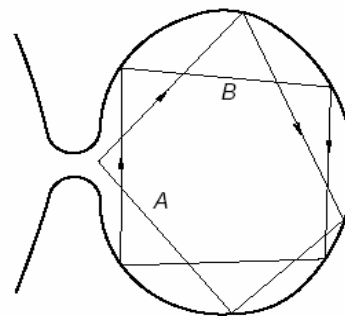
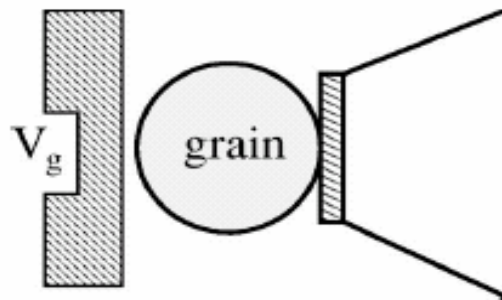
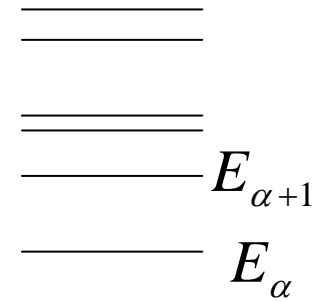
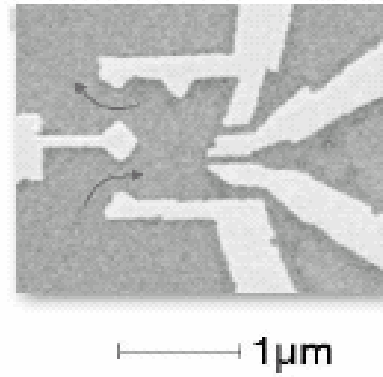
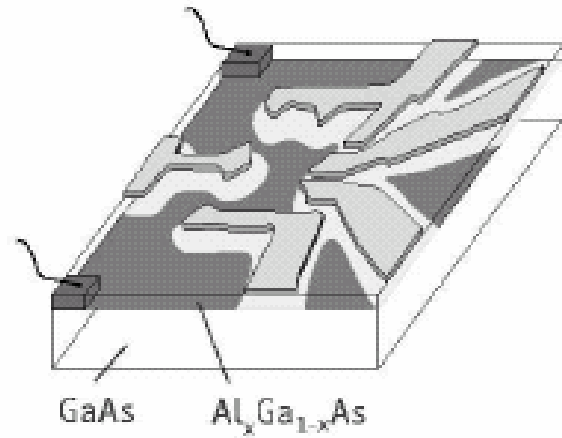
Inelastic

Electron-like
co-tunneling

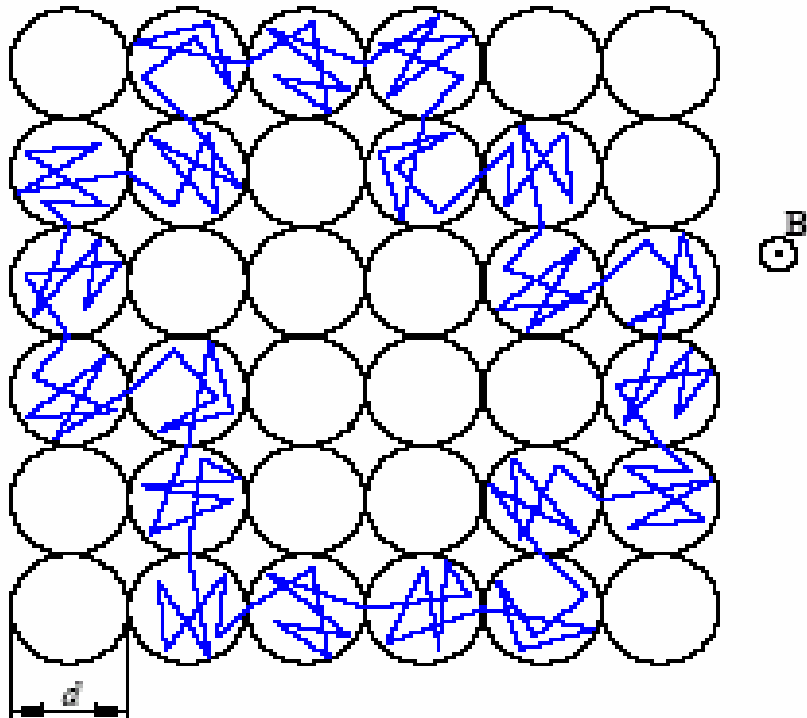
Hole-like



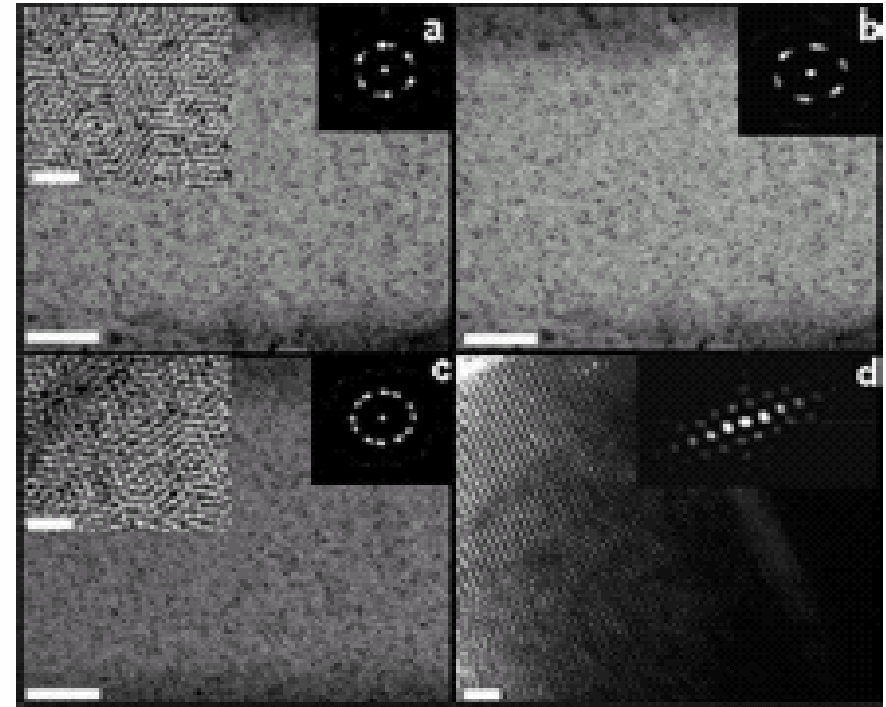
Quantum Dots with many electrons



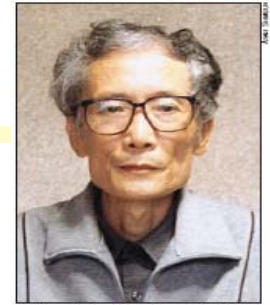
From Quantum Dots to Nano-Crystals



$d \approx 6nm$

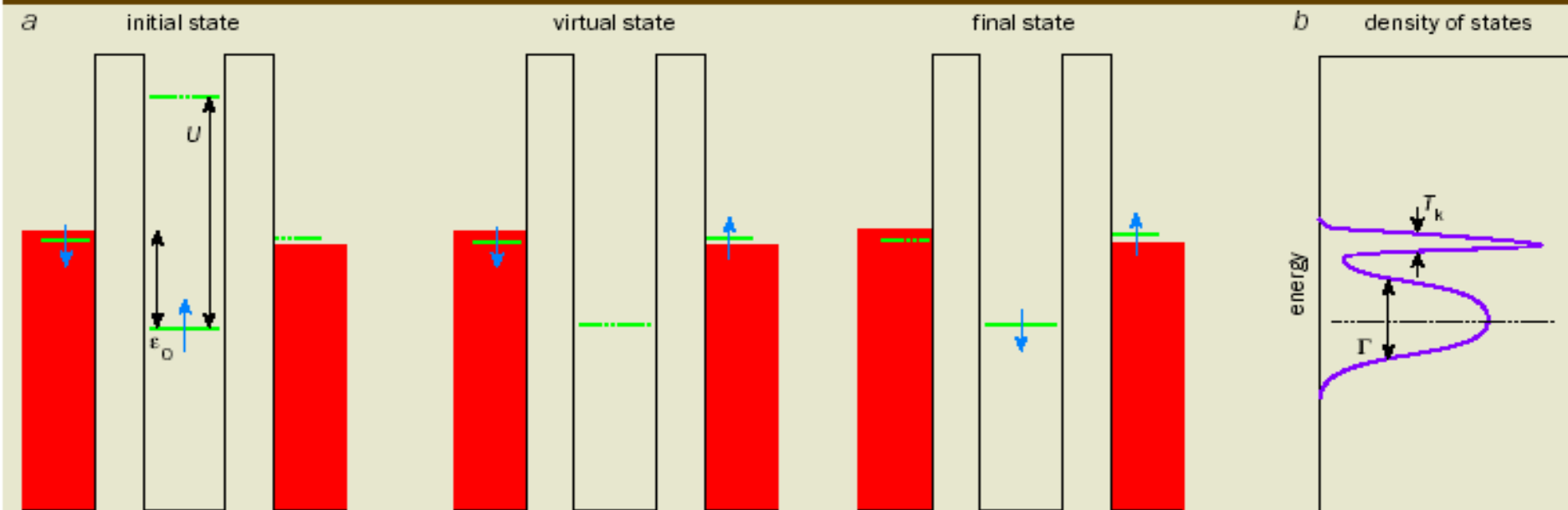


Material: Au in Si_3N_4 substrate



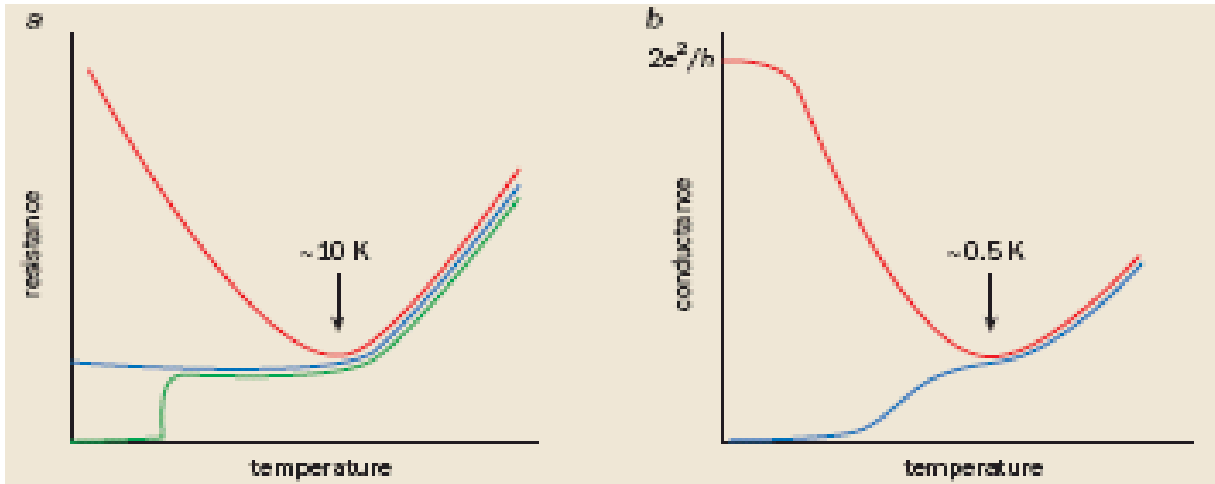
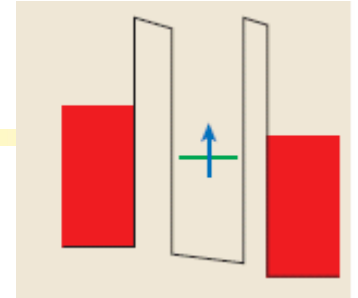
Kondo Effect in Quantum Dots

2 Spin flips



(a) The Anderson model of a magnetic impurity assumes that it has just one electron level with energy ϵ_0 below the Fermi energy of the metal (red). This level is occupied by one spin-up electron (blue). Adding another electron is prohibited by the Coulomb energy, U , while it would cost at least $|\epsilon_0|$ to remove the electron. Being a quantum particle, the spin-up electron may tunnel out of the impurity site to briefly occupy a classically forbidden "virtual state" outside the impurity, and then be replaced by an electron from the metal. This can effectively "flip" the spin of the impurity. (b) Many such events combine to produce the Kondo effect, which leads to the appearance of an extra resonance at the Fermi energy. Since transport properties, such as conductance, are determined by electrons with energies close to the Fermi level, the extra resonance can dramatically change the conductance.

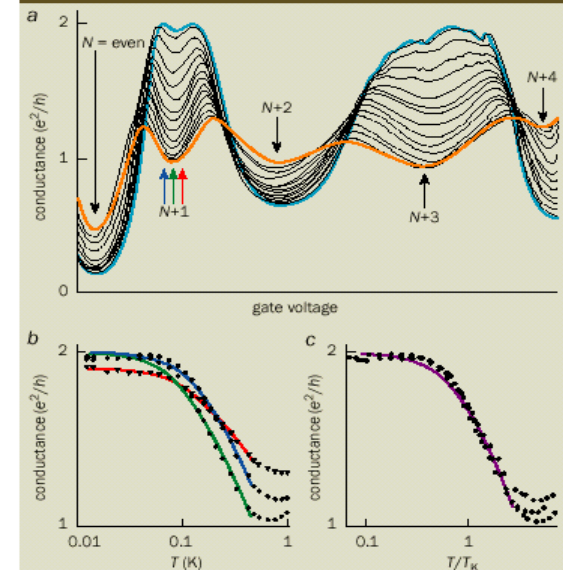
Universal Scaling



$$G / G_0 \propto \ln^{-2} (\max[T / T_K])$$

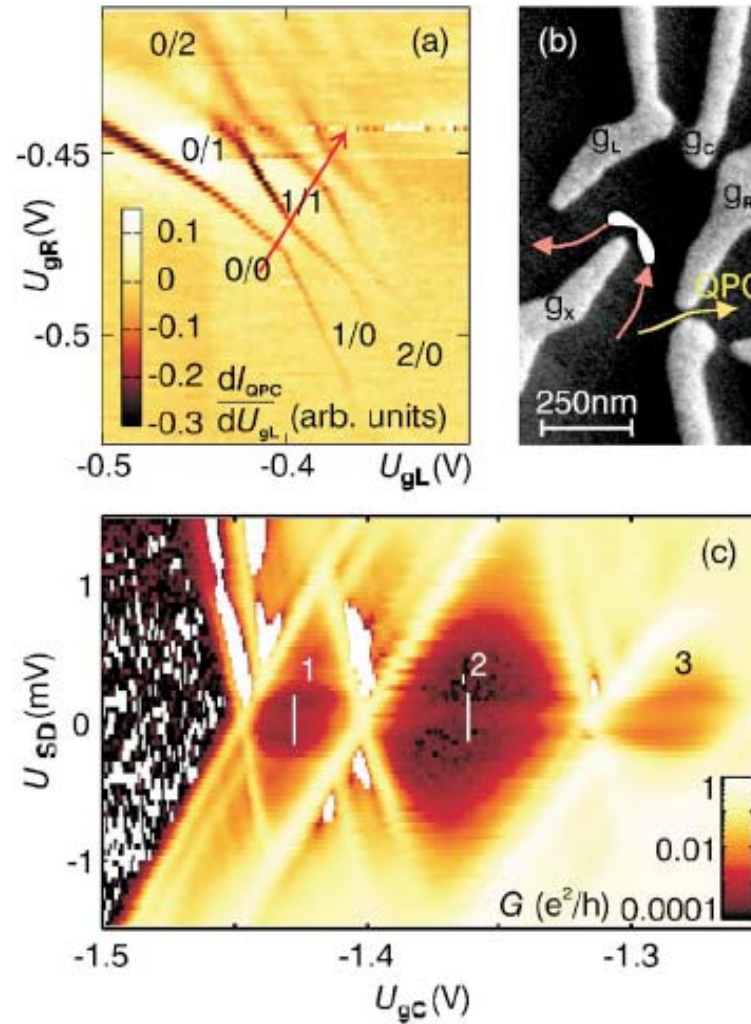
$$T_K = \frac{1}{2} (\Gamma U)^{1/2} \exp \left(\pi \epsilon_0 \frac{\epsilon_0 + U}{\Gamma U} \right)$$

5 Universal scaling

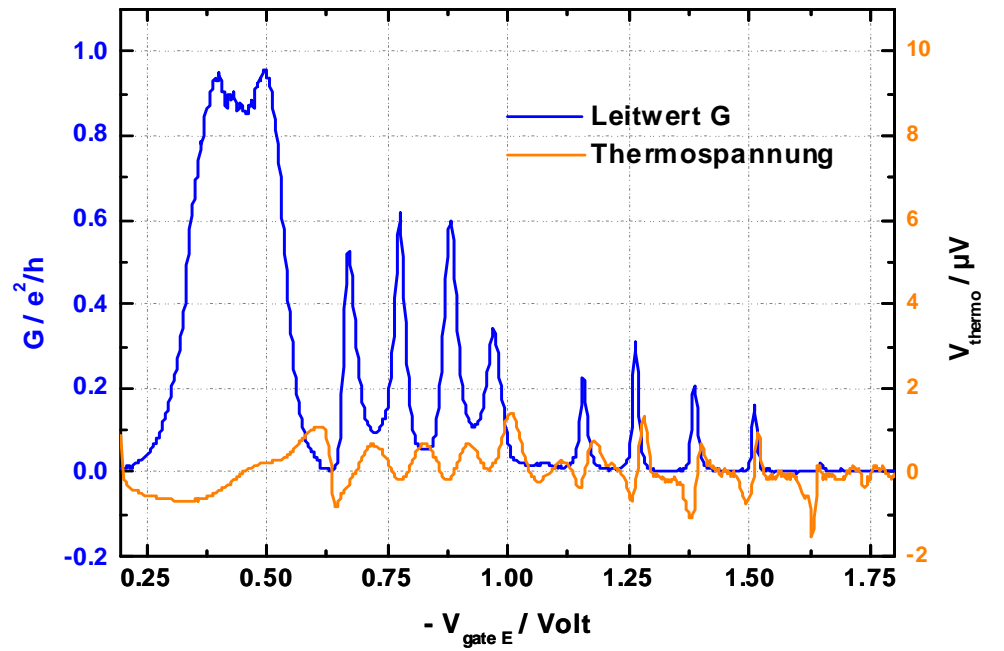
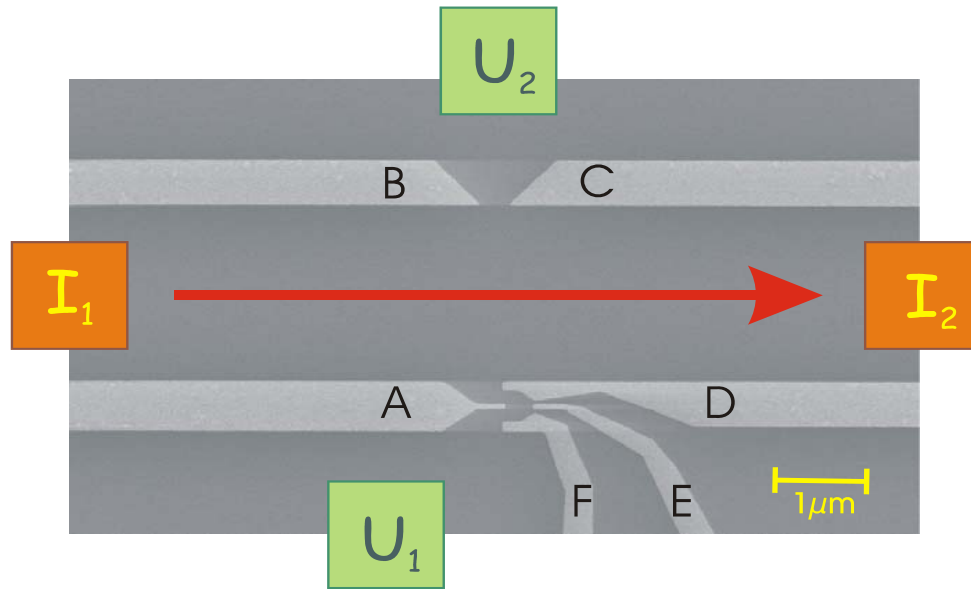
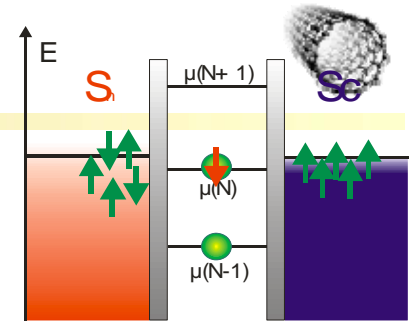


(a) The conductance (y-axis) as a function of the gate voltage, which changes the number of electrons, N , confined in a quantum dot. When an even number of electrons is trapped, the conductance decreases as the temperature is lowered from 1 K (orange) to 25 mK (light blue). This behaviour illustrates that there is no Kondo effect when N is even. The opposite temperature dependence is observed for an odd number of electrons, i.e. when there is a Kondo effect. (b) The conductance for $N + 1$ electrons at three different fixed gate voltages indicated by the coloured arrows in (a). The Kondo temperature, T_K , for the different gate voltages can be calculated by fitting the theory to the data. (c) When the same data are replotted as a function of temperature divided by the respective Kondo temperature, the different curves lie on top of each other, illustrating that electronic transport in the Kondo regime is described by a universal function that depends only on T/T_K .

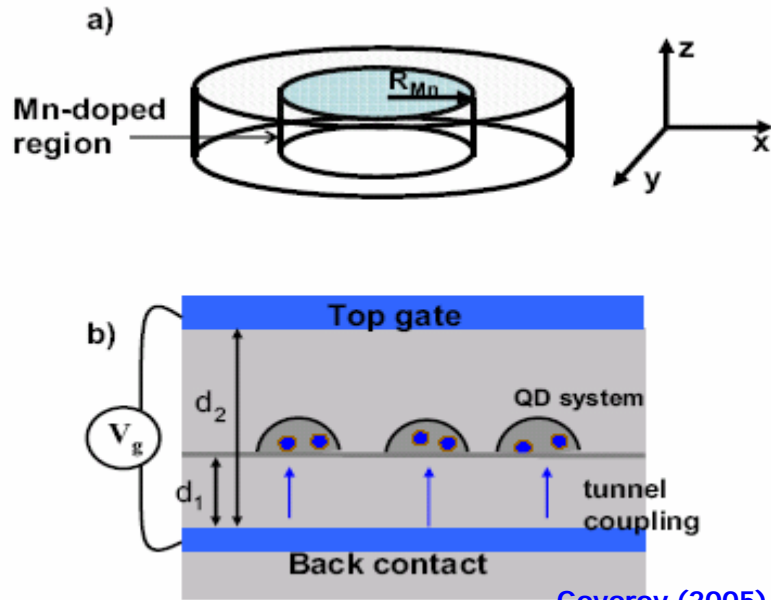
Focusing and Magnetic Control



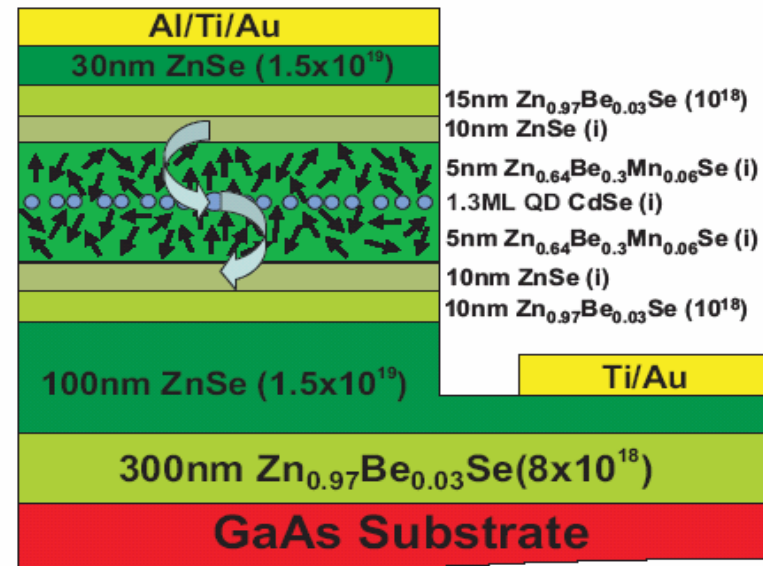
Thermo-electric properties of quantum dot



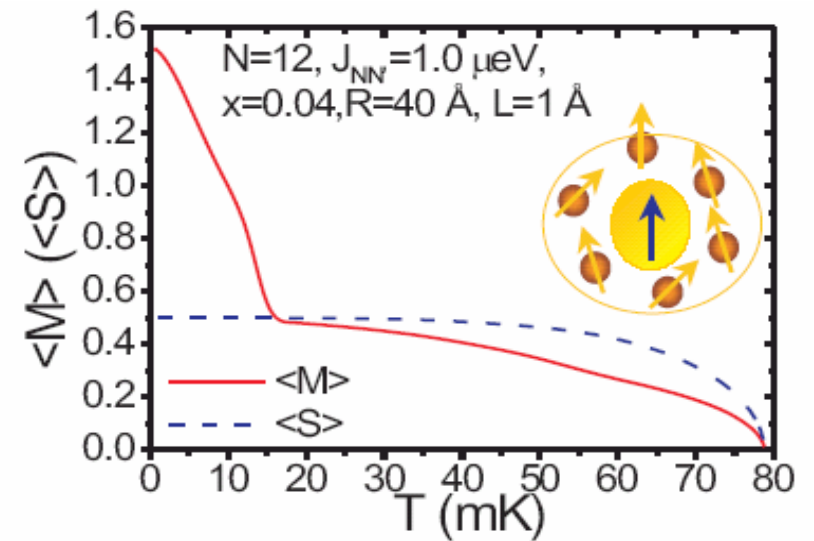
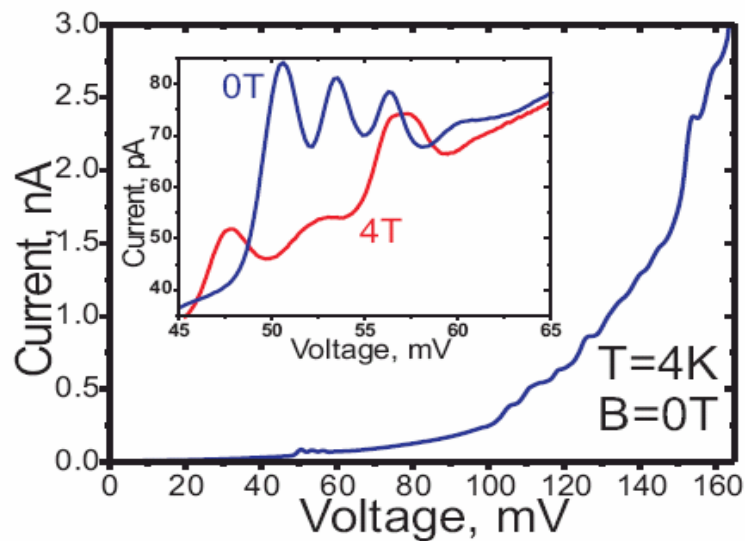
Self-assembled quantum dots



Govorov (2005)



Molenkamp et al (2005)



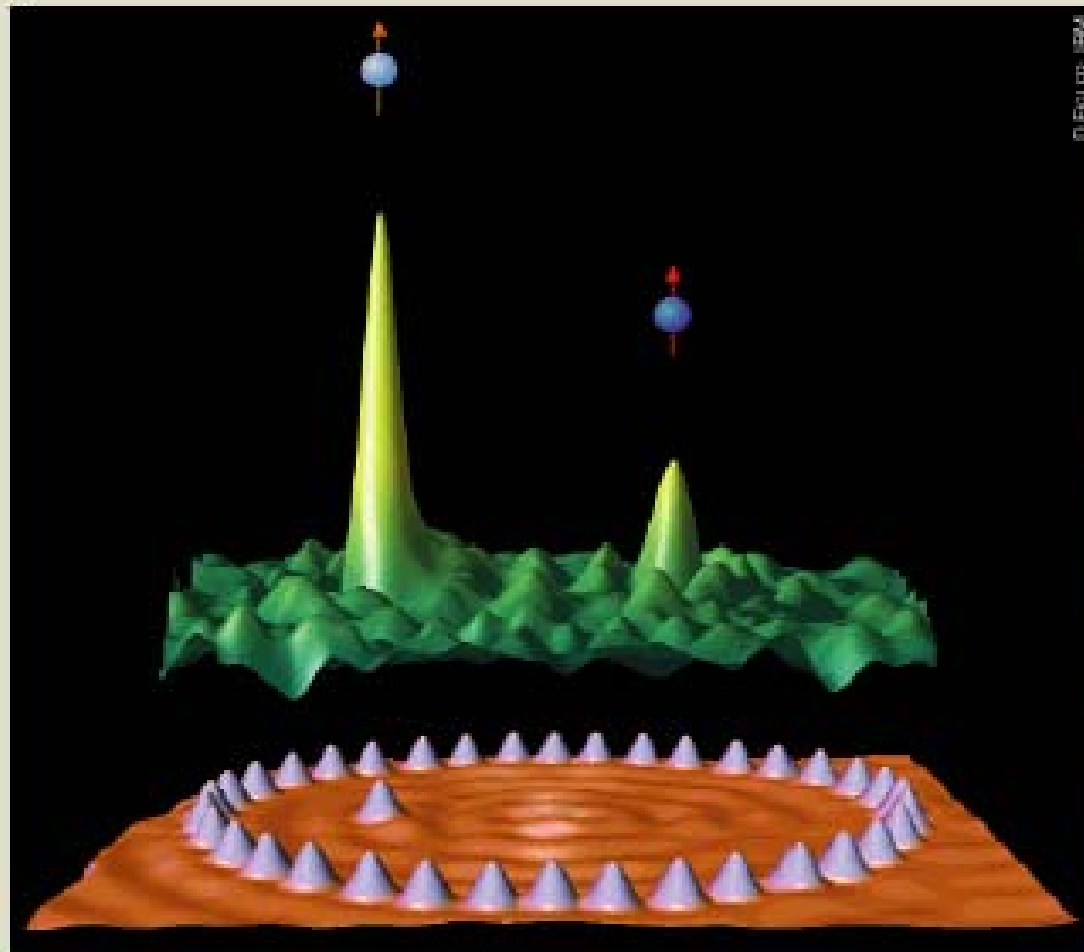


Quantum Corals

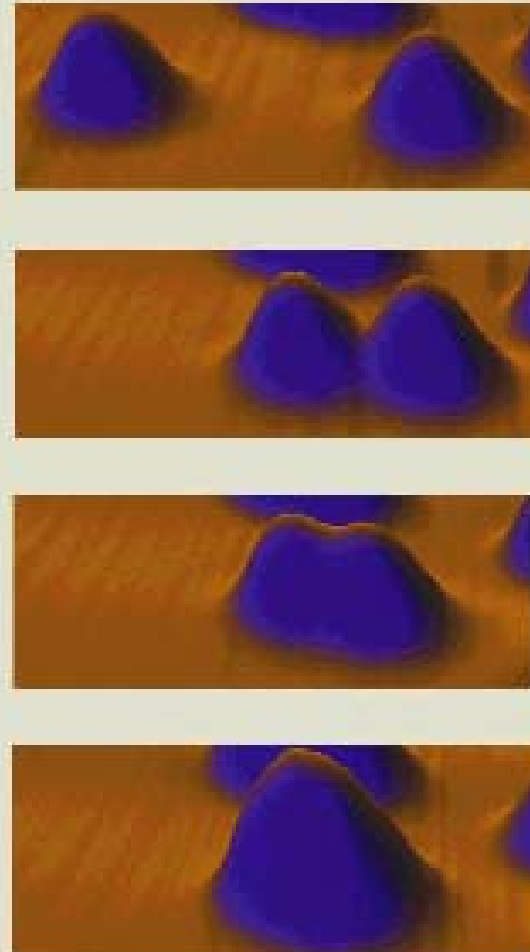
3 Single magnetic impurities under the microscope



a



b



(a) By manipulating cobalt atoms on a copper surface, Don Eigler and colleagues at IBM have placed a single cobalt atom at the focal point of an ellipse built from other cobalt atoms (bottom). The density of states (top) measured at this focus reveals the Kondo resonance (left peak). However, elliptical confinement also gives rise to a second smaller Kondo resonance at the other focal point (right) even though there is no cobalt atom there. (b) Meanwhile, Mike Crommie and co-workers have measured two Kondo resonances produced by two separate cobalt atoms on a gold surface (top). When two cobalt atoms are moved close together using an STM, the mutual interaction between them causes the Kondo effect to vanish (data not shown).

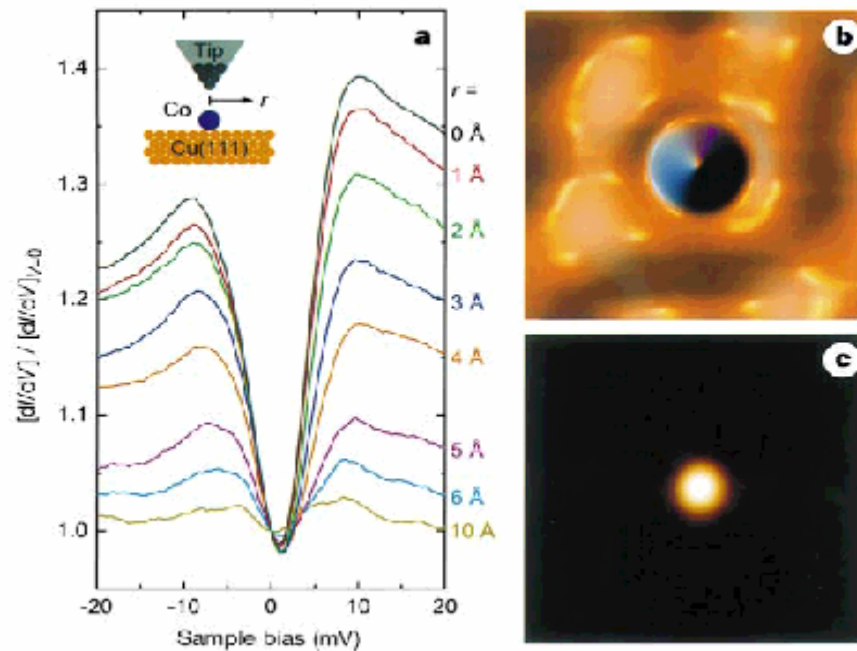


Figure 1 Detection of the Kondo resonance localized around a single Co atom on Cu(111). **a**, Tunnel spectra (normalized dI/dV) acquired over the Co atom for increasing lateral displacement r ($R_T = 100 \text{ M}\Omega$ at $V = 10 \text{ mV}$). Inset, measurement geometry. **b**, $35\text{-}\text{\AA}$ square topograph ($V = 5 \text{ mV}$, $I = 1 \text{ nA}$) of an isolated Co atom ($0.8\text{-}\text{\AA}$ -high central bump) **c**, dI/dV map of the same area (average of $V = \pm 5 \text{ mV}$ acquisitions, $V_{\text{a.c.}} = 1 \text{ mV r.m.s.}$, $I = 1 \text{ nA}$). Dark to light corresponds to increasing conductance. Examples of the three types of data obtained in this experiment: (1) Topograph images (**b**) were acquired with the scanning tunnelling microscope (STM) operating in constant d.c. current (I) mode, in which a closed feedback loop constantly adjusted tip height. (2) Tunnel spectra (**a**) were acquired by adding a small a.c. modulation $V_{\text{a.c.}}$ (1 mV r.m.s. at 201 Hz) to the d.c. bias V , opening the feedback loop (hence, holding the tip motionless with respect to the surface), and measuring dI/dV versus V through lock-in detection of the a.c. component of the tunnel current. Such spectra were essentially independent of the tunnel junction impedance R_T , determined by V/I before opening the feedback loop. (3) dI/dV image maps (**c**) were acquired simultaneously with associated topographs by applying an a.c. modulation (typically $250 \mu\text{V}$ to 1 mV r.m.s. at 201 or 1007 Hz) at a frequency exceeding the bandwidth of the feedback loop, and recording the lock-in detected dI/dV (conductance map) along with tip height (topograph) at fixed d.c. bias V while the tip was scanned in closed-loop constant- I mode. Both kinds of differential conductance measurements constitute a probe of the local density of states under the tip^{17,18}.

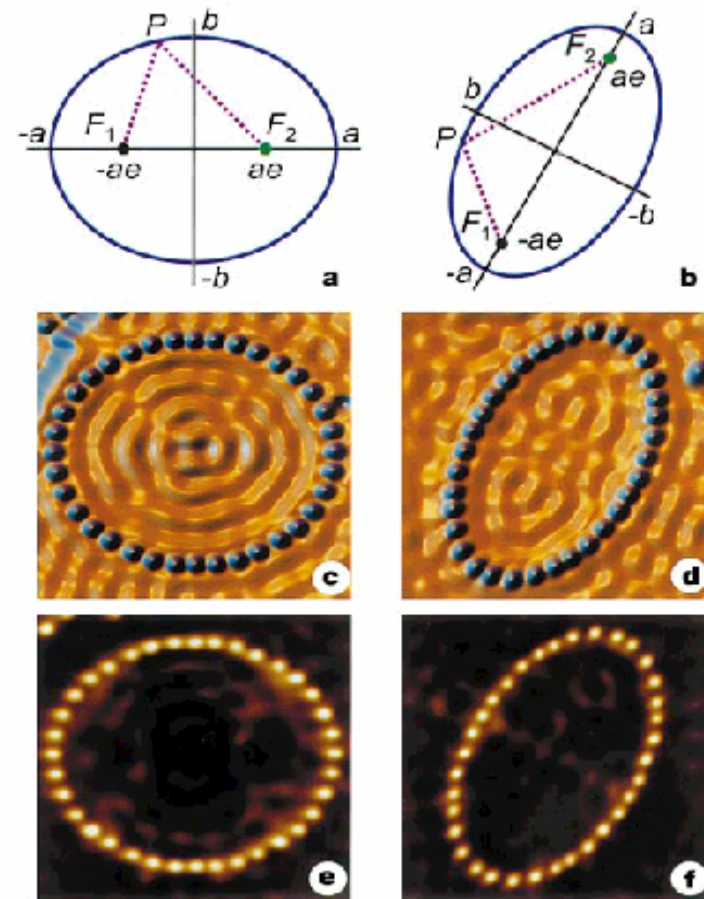
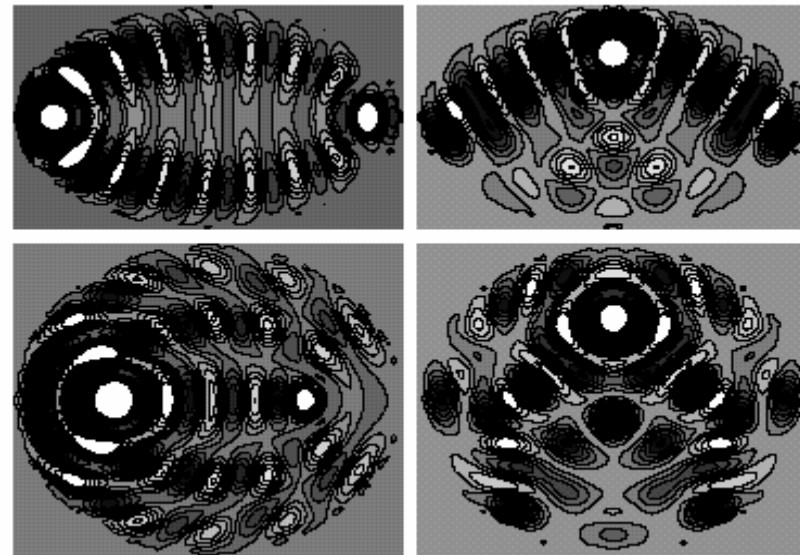
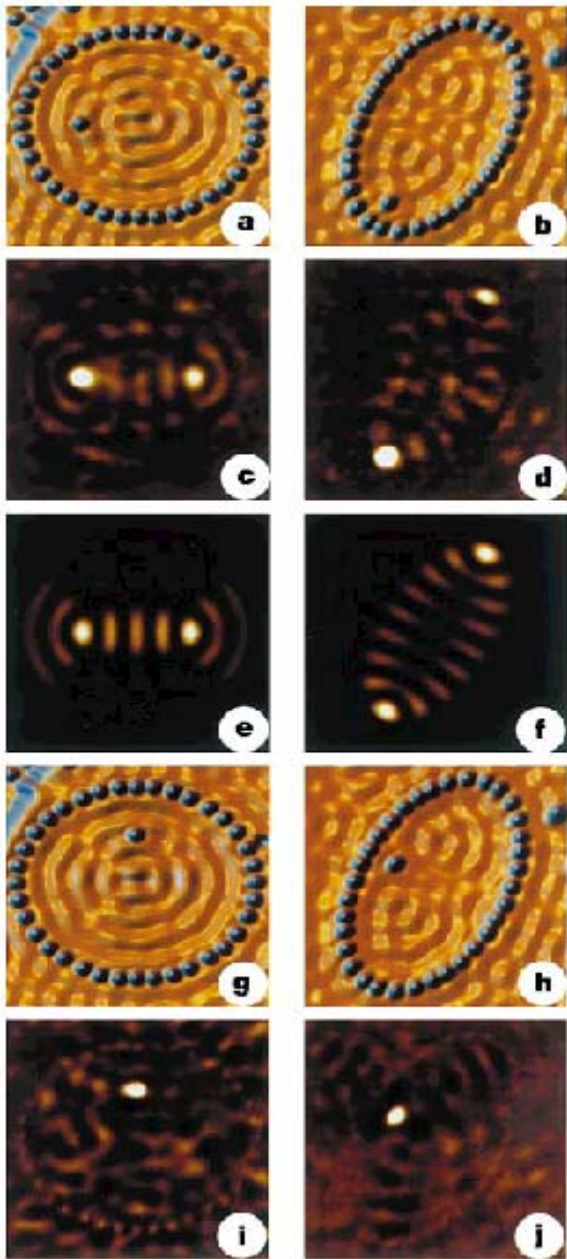


Figure 2 Elliptical electron resonators. **a**, Eccentricity $e = 1/2$; **b**, $e = 0.786$. **c**, **d**, Corresponding topographs of the experimental realizations ($a = 71.3 \text{\AA}$ for both ellipses) employing Co atoms to corral two-dimensional electrons on Cu(111). **e**, **f**, dI/dV maps acquired simultaneously with the corresponding topographs, tuned to image the Kondo resonance. ($V = 10 \text{ mV}$, $V_{\text{a.c.}} = 250 \mu\text{V r.m.s.}$, $I = 1 \text{ nA}$ for **c** and **e**; $V = 8 \text{ mV}$, $V_{\text{a.c.}} = 1 \text{ mV r.m.s.}$, $I = 1 \text{ nA}$ for **d** and **f**). Image dimensions are 150\AA square and 154\AA square for the $e = 1/2$ and $e = 0.786$ ellipses, respectively.

H.Manoharan et al, Nature 403, 512 (2002)



$$\delta\rho(\vec{R}, \epsilon_F) \simeq \rho_0 \frac{16t^3}{(k_F d)^2} \cos(4k_F a).$$

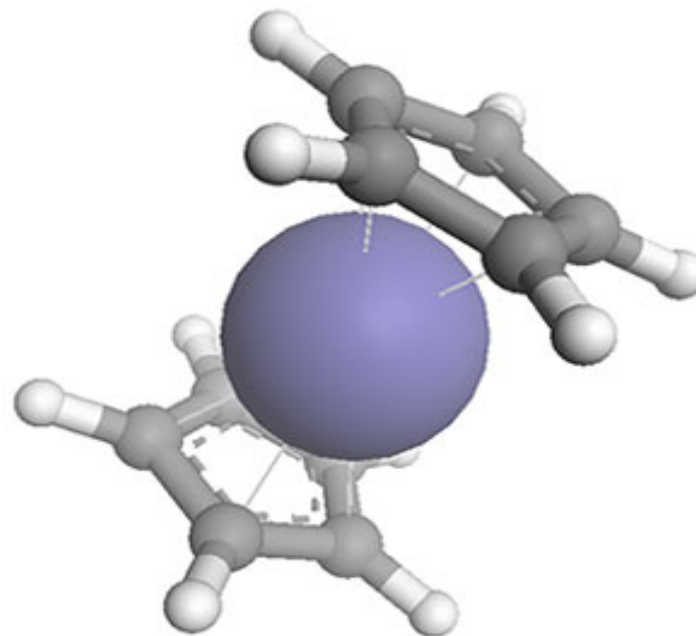
Figure 3 Visualization of the quantum mirage. **a, b**, Topographs showing the $e = 1/2$ (**a**) and $e = 0.786$ (**b**) ellipse each with a Co atom at the left focus. **c, d**, Associated dI/dV difference maps showing the Kondo effect projected to the empty right focus, resulting in a Co atom mirage. **e** and **f**, Calculated eigenmodes at E_- (magnitude of the wavefunction is plotted). When the interior Co atom is moved off focus (**g** and **h**, topographs), the mirage vanishes (**i** and **j**, corresponding dI/dV difference maps). Imaging conditions and dimensions as in Fig. 2. We have assembled over 20 elliptical resonators of varying size and eccentricity and searched for the formation of a quantum mirage. We find that as a is increased monotonically while e is fixed, the mirage is switched on and off. In each period of this switching, the classical path length $2a$ changes by a half Fermi wavelength. Because we also observe that two focal atoms, one on each focus, couple quite strongly with one another (as judged by the perturbation of the Kondo resonance) these oscillatory



Molecular Transistors

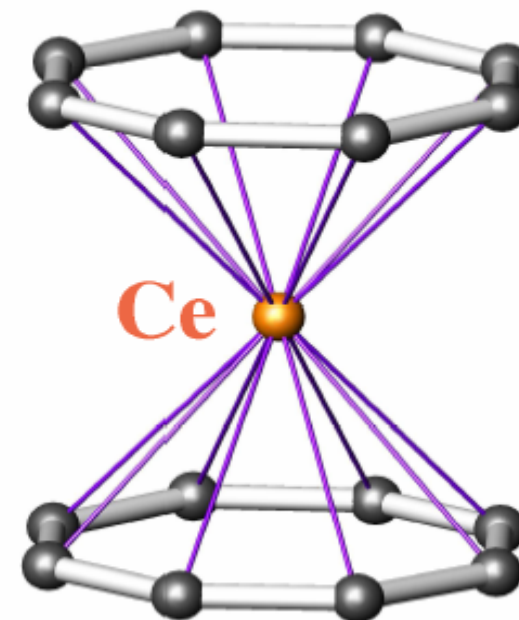


Ferrocene





Cerocene

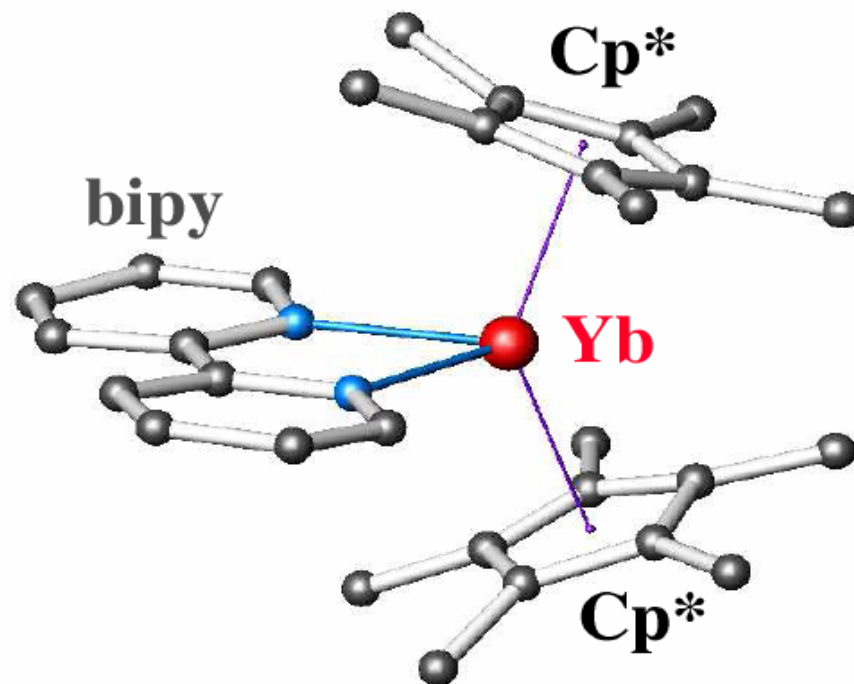


COT

COT = C₈H₈



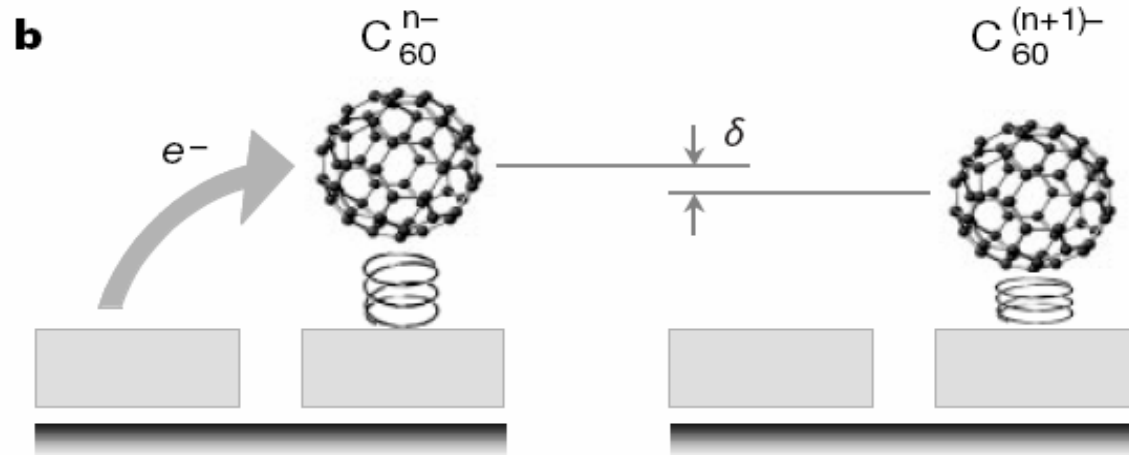
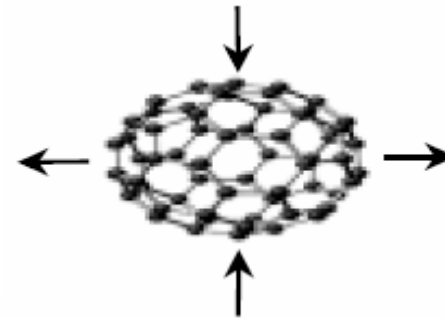
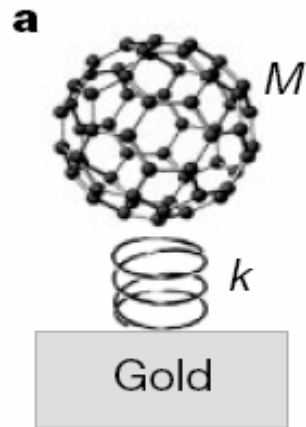
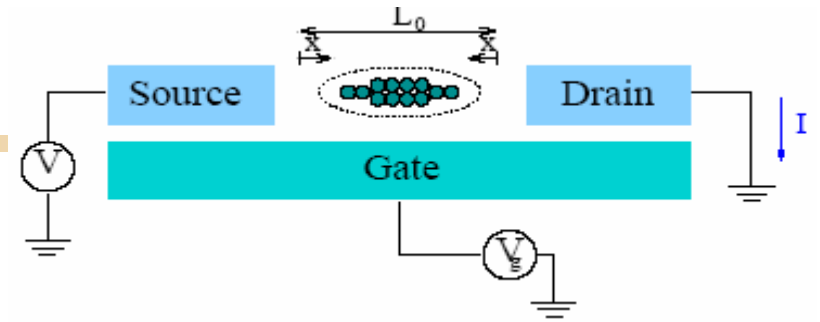
Ytterbocene



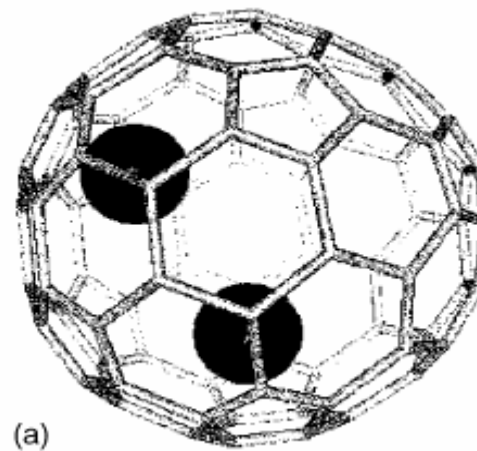
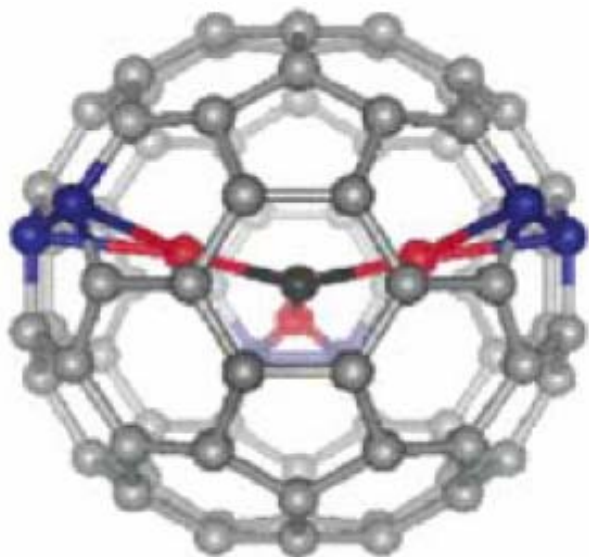
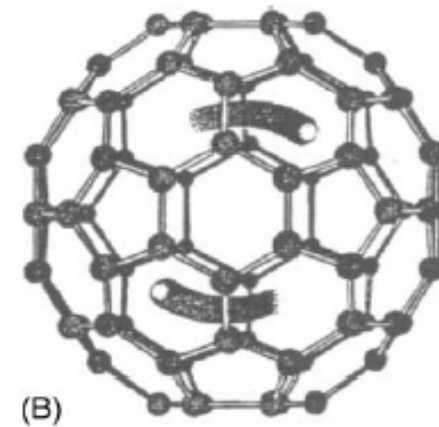
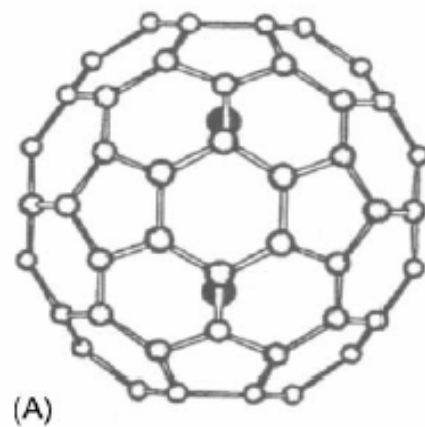
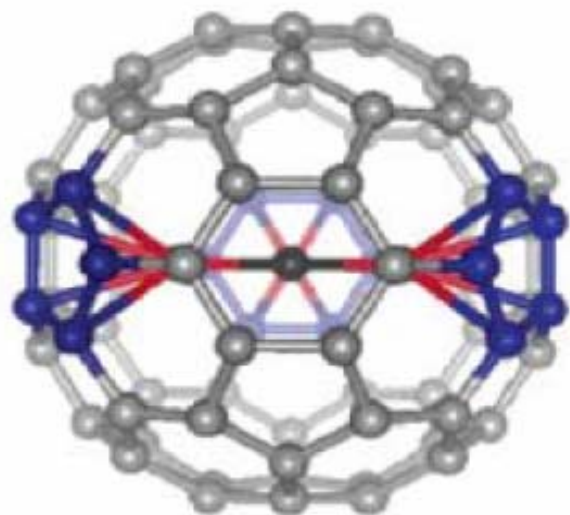
$\text{Cp}^* = \text{C}_5\text{Me}_5$,

$\text{bipy} = (\text{NC}_5\text{H}_4)_2$

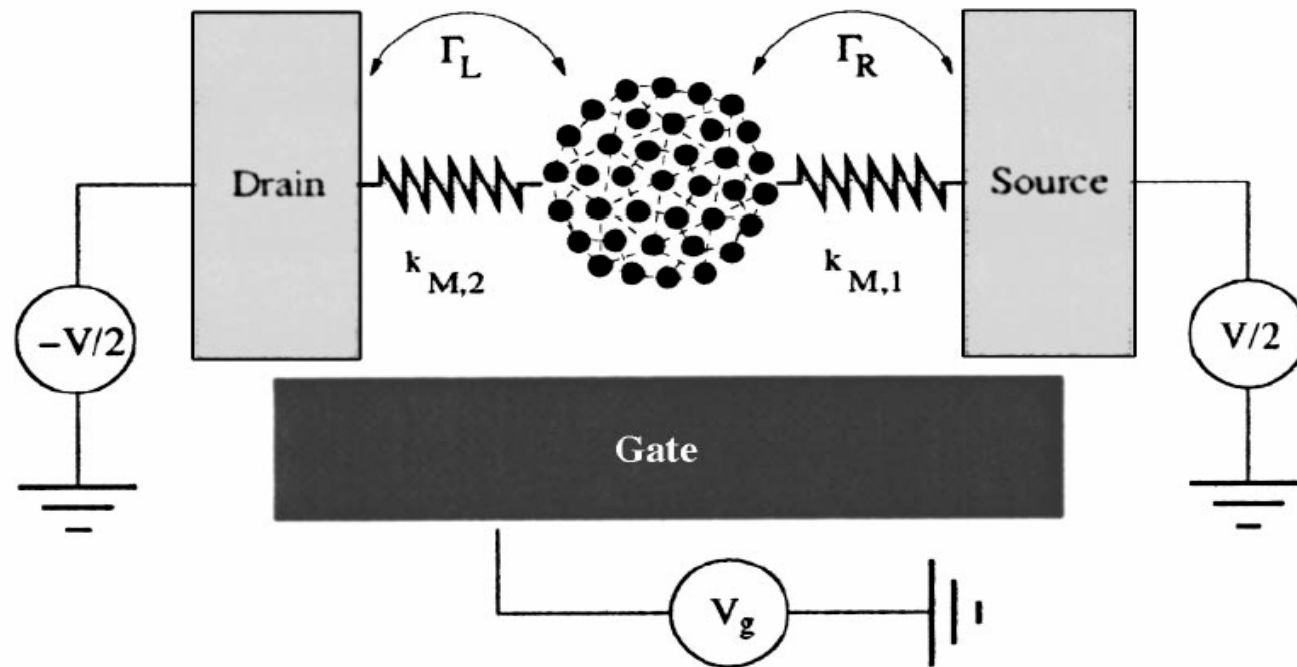
Fullerenes



Transition metals inside fullerenes



Transport through molecular transistors





Nano Electro Mechanics

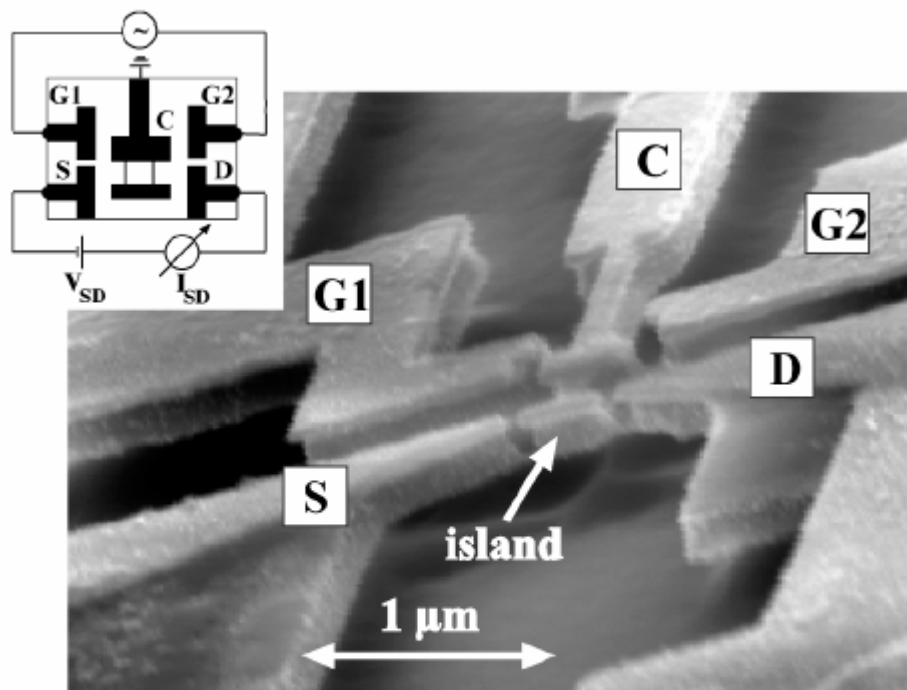


FIG. 1. Electron micrograph of the quantum bell: The pendulum is clamped on the upper side of the structure. It can be set into motion by ac power, which is applied to the gates on the left- and right-hand sides (G1 and G2) of the clapper (C).

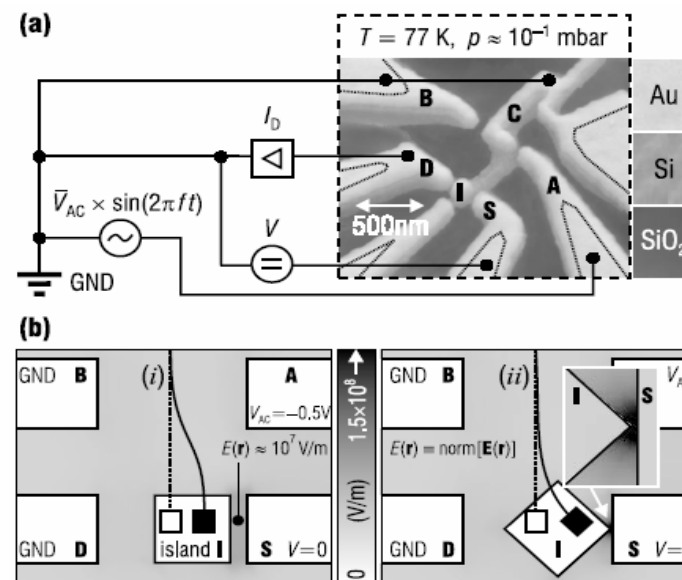
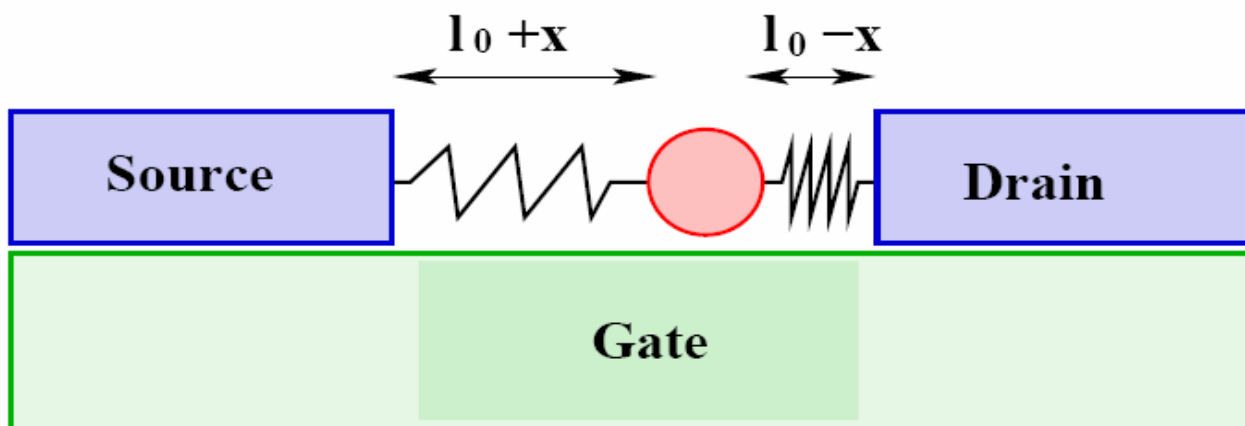


FIG. 1. (a) Scanning electron microscopy micrograph and experimental setup of the device: the electron shuttle consists of a gold island I situated at the end of a nanomachined silicon cantilever. Free suspension outside the area marked by the dotted lines is ~ 200 nm. The island oscillates between source S and drain D, where the current I_D is detected via a current ampli-



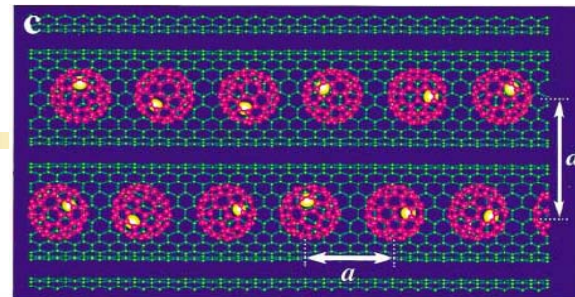
Nanoelectromechanical shuttling. Schematic concept (NEMS)



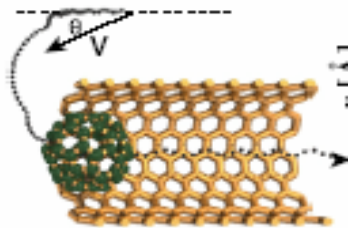
More complicated object à la H_2 molecule:



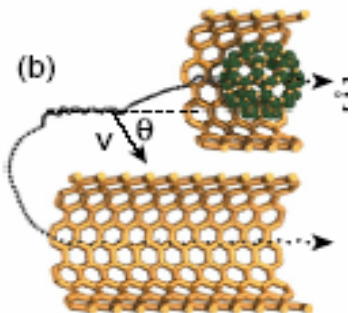
Nanotube peapods: C_{60} @ CNT



(a)



(b)



(c)

